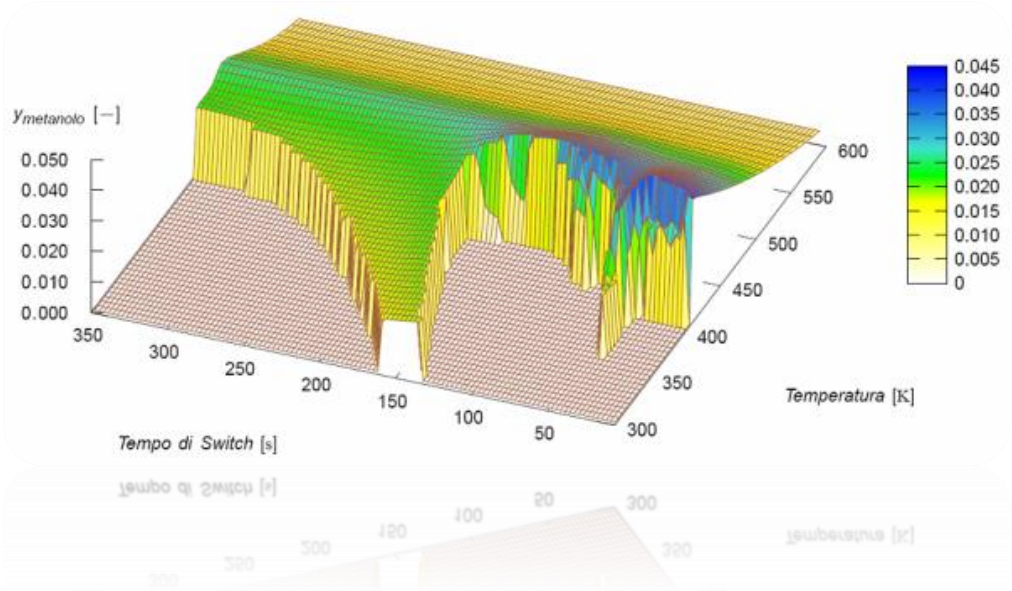

Dynamics of forced and unsteady-state processes

Davide Manca

Lesson 3 of "Dynamics and Control of Chemical Processes" – Master Degree in Chemical Engineering

POLITECNICO
MILANO 1863

Forced unsteady-state reactors

- Forced unsteady state (FUS) reactors allow reaching higher conversions than conventional reactors.
- Two alternatives:
  - Reverse flow reactors, **RFR**;
  - Network of reactors: simulated moving bed reactors, **SMBR**.
- Within a **SMBR** network, the simulated moving bed is accomplished by periodically switching the feed inlet from one reactor to the following one.
- **APPLICATION**: Methanol synthesis (ICI patent).
  - Operating temperature: 220-300 °C;
  - Pressure: 5-8 MPa;
  - CO = 10-20%; CO_2 = 6-10%; H_2 = 70-80%.

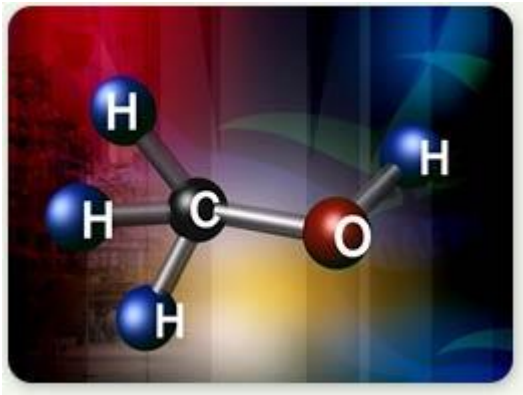

Forced unsteady-state reactors

- Catalytic exothermic reactions can be carried out with an autothermal regime.
- FUS reactors are mainly advantageous when either the reactants concentration or the reactions exothermicity are low.
- There is an increase of both conversion and productivity that allows:
  - Using smaller reactors,
  - Lower amounts of catalyst.

Methanol synthesis in forced unsteady-state reactors

- The methanol synthesis reaction is:

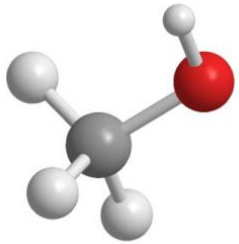

$$CO + 2H_2 \rightleftarrows CH_3OH \qquad \Delta\tilde{H}_R = -90.769 \text{ kJ/mol}$$

- The reaction takes place with a reduction of the moles number. Therefore, the reaction is carried out at high pressure.
- In the past, the methanol plants worked at 100 ÷ 600 bar.
- Nowadays, methanol plants work at lower pressures (50 – 80 bar).
- In the low-pressure plants, the following reactions are important too:

$$CO_2 + H_2 \rightleftarrows CO + H_2O$$
$$CO_2 + 3H_2 \rightleftarrows CH_3OH + H_2O$$

Reverse Flow Reactors

- Valves: V_1, V_2, V_3, V_4 allow periodically inverting the feed direction in the reactor.

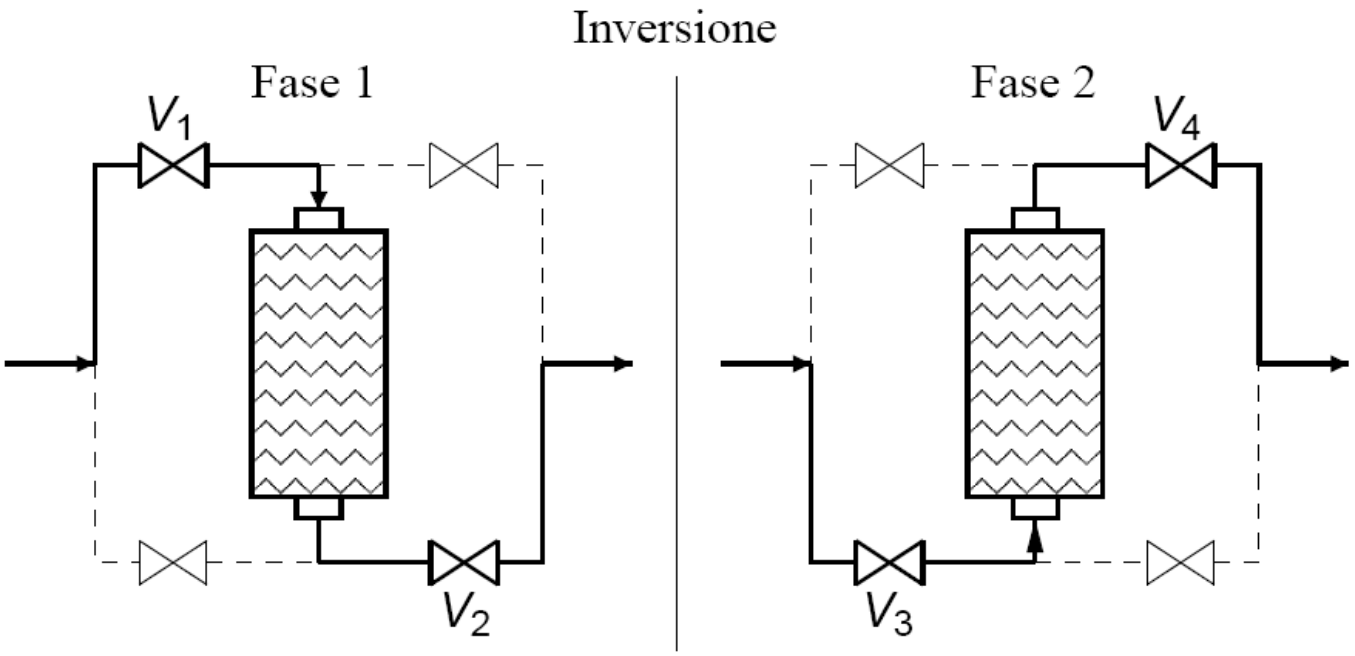

RFR: first–principles model

Equations	#Eq.	Eq. type	Variables
Gas phase enthalpic balance	1	Partial derivative	$T_G, T_S, \underbrace{y_{G,i}}_{i=1...nComp}$
Solid phase enthalpic balance (catalyst)	1	Partial derivative	$T_G, T_S, \underbrace{y_{G,i}}_{i=1...nComp}, \underbrace{y_{S,i}}_{i=1...nComp}$
Gas phase material balance	nComp	Partial derivative	$T_G, T_S, \underbrace{y_{G,i}}_{i=1...nComp}, \underbrace{y_{S,i}}_{i=1...nComp}$
Solid phase material balance (catalyst)	nComp	Non-linear algebraic	$T_G, T_S, \underbrace{y_{G,i}}_{i=1...nComp}, \underbrace{y_{S,i}}_{i=1...nComp}$

$2\,nComp + 2$ $\qquad$ $2\,nComp + 2$

RFR: methanol synthesis

Reactor diameter	D_R	0.1	[m]
Reactor length	L	0.5	[m]
Void fraction	ϵ	0.4	[−]
Catalyst mass	W	41.2	[kg]
Apparent catalyst density	ρ_S	1750	[kg/m^3]
Catalyst porosity	ϵ_S	0.5	[−]
Pellet diameter	d_p	0.0054	[m]
Inlet temperature	T_{in}	373.15	[K]
Working pressure	P	5	[MPa]
Surface flowrate	F_{in}	32.65	[mol/m^2/s]

RFR: methanol synthesis

Specie nel gas in ingresso	Frazione molare
CO	0.045
CO_2	0.02
H_2	0.935

Tipologia catalizzatore	$Cu/Zn/Al_2O_3$ oppure $Cu/Zn/Cr_2O_3$
Contenuto di CuO	$50\% \div 70\%$
Contenuto di ZnO	$20\% \div 30\%$
Durata	circa 2 anni
Cause disattivazione	presenza di zolfo sinterizzazione Cu ($T > 573\,\mathrm{K}$)

Reverse Flow Reactors

Temperature profile once the pseudo-stationary condition is reached

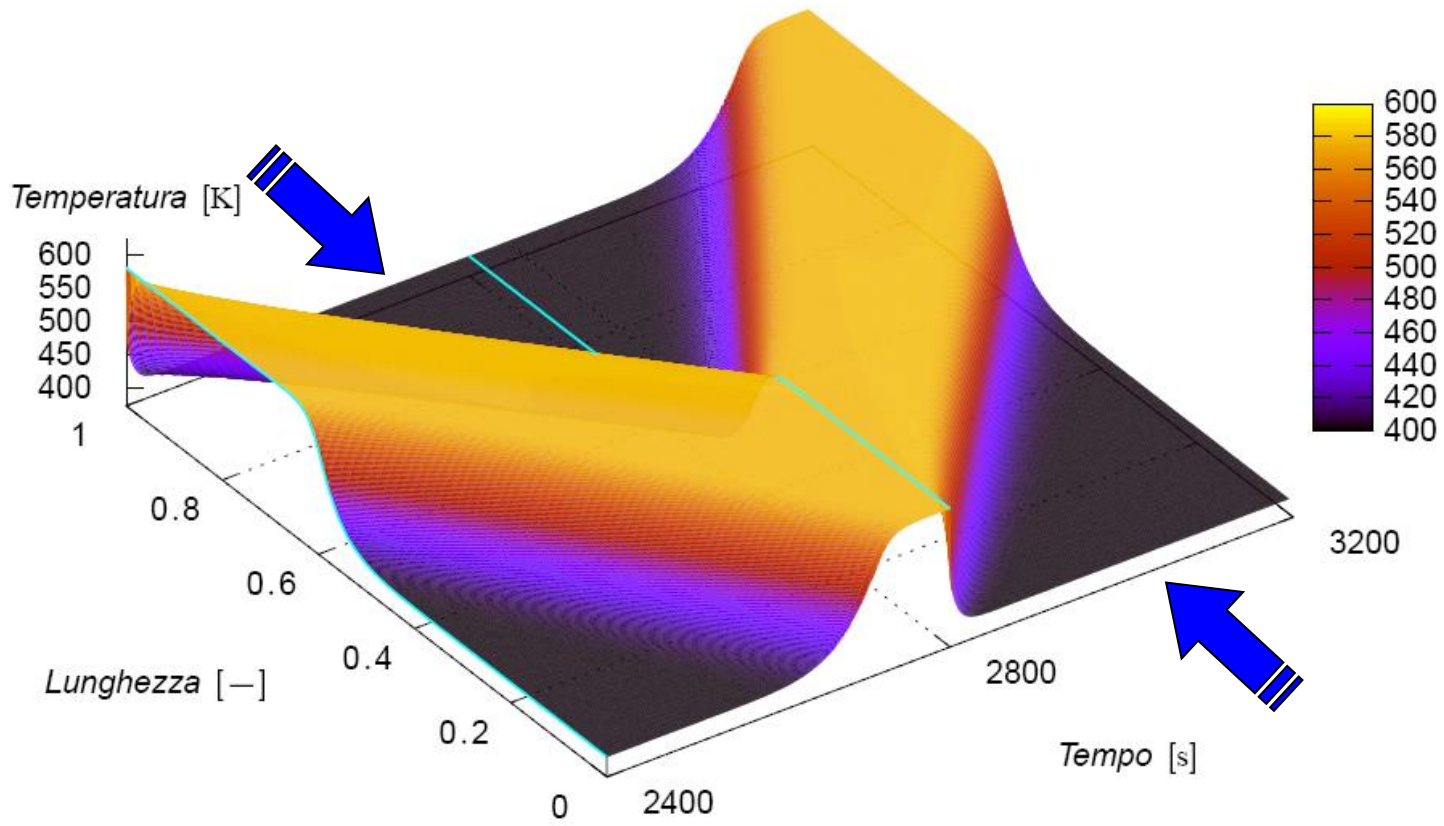

Reverse Flow Reactors

Concentration profile once the pseudo-stationary condition is reached

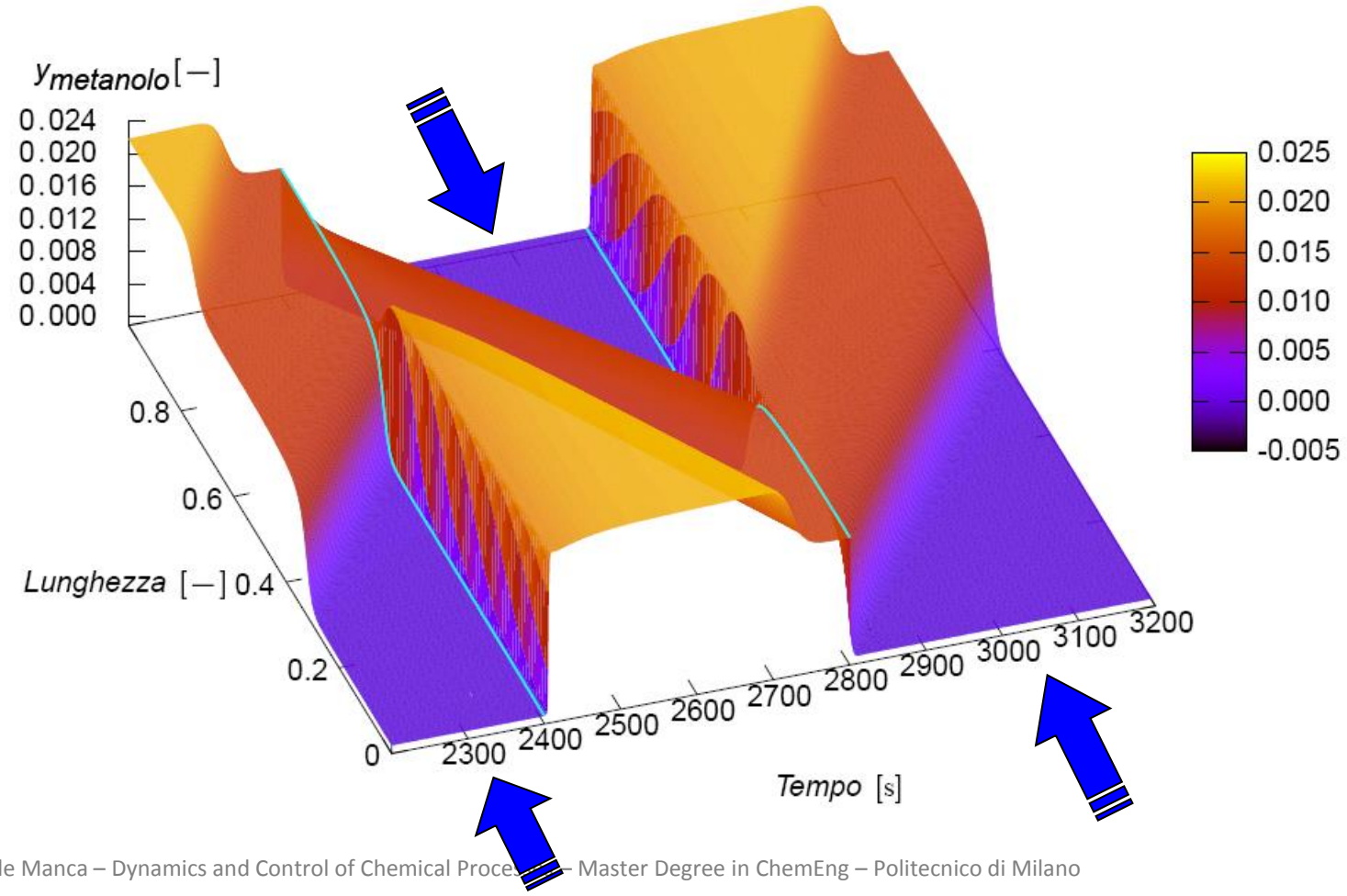

Simulated Moving Bed Reactors

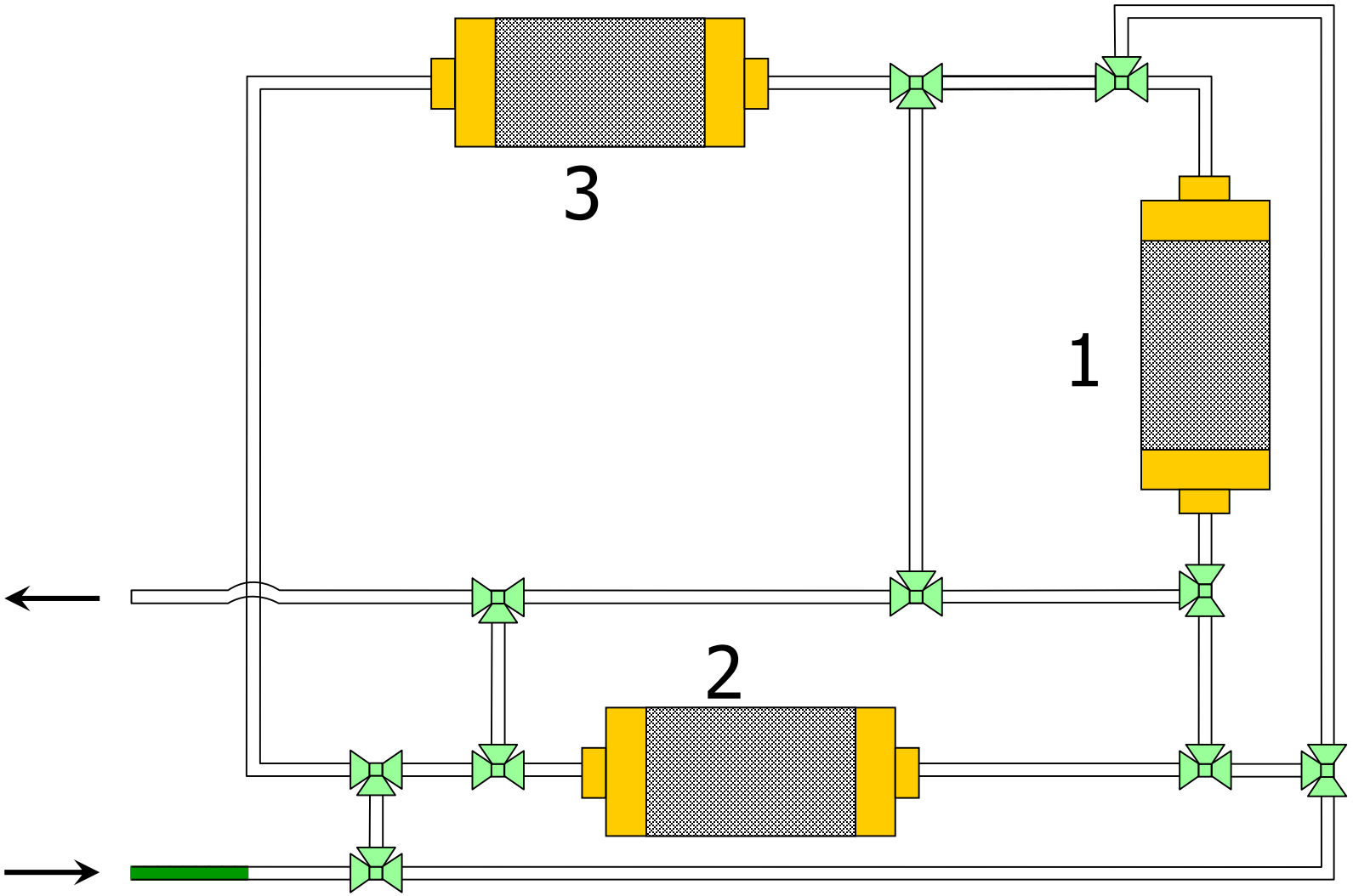

Step 3: 3→1→2

Simulated Moving Bed Reactors

- Continuity equation for the gas phase:

$$\frac{\partial c_G}{\partial t} + \frac{\partial}{\partial x} c_G v = \sum_{i=1}^{n_r} \frac{k_{G,i} a_v}{\varepsilon} (y_{S,i} - y_{G,i}). \quad (1)$$

- Continuity equation for component j in the gas phase:

$$\frac{\partial y_{G,j}}{\partial t} = D_{eff} \frac{\partial^2 y_{G,j}}{\partial x^2} - v \frac{\partial y_{G,j}}{\partial x} + \frac{k_{G,j} a_v}{c_G \varepsilon} (y_{S,j} - y_{G,j}) - y_{G,j} \sum_{i=1}^{n_r} \frac{k_{G,i} a_v}{c_G \varepsilon} (y_{S,i} - y_{G,i})$$

$$\text{with } j = 1, \ldots, (n_r - 1). \quad (2)$$

- Energy balance for the gas phase:

$$\frac{\partial T_G}{\partial t} = \frac{k_{eff}}{\varrho \hat{c}_{P,G}} \frac{\partial^2 T_G}{\partial x^2} - v \frac{\partial T_G}{\partial x} + \frac{h a_v}{\varrho \hat{c}_{P,G} \varepsilon} (T_S - T_G). \quad (3)$$

- Mass balance for the solid phase:

$$k_{G,j} a_v (y_{S,j} - y_{G,j}) = [\varrho_S (1 - \varepsilon)] \sum_{k=1}^{N_R} \eta_k \nu_{j,k} R'_k$$

$$\text{with } j = 1, \ldots, n_r. \quad (4)$$

- Energy balance for the solid phase:

$$\frac{\partial T_S}{\partial t} = \frac{\lambda_S}{\varrho_S \hat{c}_{P,S}} \frac{\partial^2 T_S}{\partial x^2} - \frac{h a_v}{\varrho_S \hat{c}_{P,S} (1 - \varepsilon)} (T_S - T_G) + \frac{1}{\hat{c}_{P,S}} \sum_{i=1}^{n_r} \left(\sum_{k=1}^{N_R} \eta_k \nu_{i,k} R'_k \right) (-\Delta \tilde{H}_{f,i}). \quad (5)$$

• Kinetic equations corresponding to a dual-site Langmuir-Hinshelwood mechanism, based on three independent reactions: methanol formation from CO, water-gas-shift reaction and methanol formation from CO2:

$$CO + 2H_2 \rightleftharpoons CH_3OH, \quad (6)$$

$$CO_2 + H_2 \rightleftharpoons CO + H_2O, \quad (7)$$

$$CO_2 + 3H_2 \rightleftharpoons CH_3OH + H_2O. \quad (8)$$

Velardi S., A. Barresi, D. Manca, D. Fissore, Chem. Eng. J., 99 117–123, 2004

Simulated Moving Bed Reactors

- Reaction rates for a catalyst based on Cu–Zn–Al mixed oxides

$$R'_{CH_3OH,A} = \frac{k'_{ps,A} K_{CO} \left[p_{CO} p_{H_2}^{3/2} - \frac{p_{CH_3OH}}{p_{H_2}^{1/2} K_{p,A}} \right]}{(1 + K_{CO} p_{CO} + K_{CO_2} p_{CO_2})[p_{H_2}^{1/2} + (K_{H_2O}/K_{H_2}^{1/2}) p_{H_2O}]}, \tag{9}$$

$$R'_{H_2O,B} = \frac{k'_{ps,B} K_{CO_2} \left[p_{CO_2} p_{H_2} - \frac{p_{H_2O} p_{CO}}{K_{p,B}} \right]}{(1 + K_{CO} p_{CO} + K_{CO_2} p_{CO_2})[p_{H_2}^{1/2} + (K_{H_2O}/K_{H_2}^{1/2}) p_{H_2O}]}, \tag{10}$$

$$R'_{CH_3OH,C} = R'_{H_2O,C} = \frac{k'_{ps,C} K_{CO_2} \left[p_{CO_2} p_{H_2}^{3/2} - \frac{p_{CH_3OH} p_{H_2O}}{(p_{H_2}^{3/2} K_{p,C})} \right]}{(1 + K_{CO} p_{CO} + K_{CO_2} p_{CO_2})[p_{H_2}^{1/2} + (K_{H_2O}/K_{H_2}^{1/2}) p_{H_2O}]}. \tag{11}$$

Concerning the gas-solid heat transfer coefficient, the following correlation has been adopted:

$$\frac{h d_P}{\lambda_G} = 1.6(2 + F Re_P^{0.5} Pr^{1/3}) \tag{12}$$

with

$$F = 0.664 \sqrt{1 + \left[\frac{0.0557 Re_P^{0.3} Pr^{2/3}}{1 + 2.44(Pr^{2/3} - 1) Re_P^{-0.1}} \right]^2} \tag{13}$$

Velardi S., A. Barresi, D. Manca, D. Fissore, Chem. Eng. J., 99 117–123, 2004

Simulated Moving Bed Reactors

The prediction of the axial heat dispersion coefficient has been carried out adopting a correlation by Dixon and Cresswell [15]:

$$\frac{k_{\text{eff}}}{\varrho v \hat{c}_{P,\text{G}} d_{\text{P}}} = \frac{0.73 + (\lambda_{\text{st}}/\lambda_{\text{G}})}{Re_{\text{P}} Pr} + \frac{0.5}{1 + 9.7(Re_{\text{P}} Pr)}, \tag{14}$$

where the term $\lambda_{\text{st}}/\lambda_{\text{G}}$ accounts for the stagnant zone contribution. According to Edwards and Richardson [16] a correlation of the same general form as Eq. (14) can be used for the prediction of mass dispersion coefficient:

$$\frac{D_{\text{eff}}}{v d_{\text{P}}} = \frac{0.73}{Re_{\text{P}} Sc} + \frac{0.5}{1 + 9.7/(Re_{\text{P}} Sc)}. \tag{15}$$

Conventional Danckwerts boundary conditions are assumed at the inlet section of the network. The continuity of the gas temperature and concentration profiles has been imposed between each reactor of the sequence, at sections $x = \ell$ and 2ℓ. In addition, spatial derivatives should vanish at the outlet sections. At time $t = 0$ the reactants concentration is null, while the initial temperatures of the gas and solid phases are the same. When the switching time is reached the origin of the x-axis moves from the first reactor of the sequence to the second one and the switching conditions are applied in order to simulate the change of the inlet position:

$$x \in]0, 2\ell[\quad \begin{cases} y_{\text{G},j}(x)|_{t+} = y_{\text{G},j}(x+\ell)|_{t-} \\ T_{\text{G}}(x)|_{t+} = T_{\text{G}}(x+\ell)|_{t-} \\ T_{\text{S}}(x)|_{t+} = T_{\text{S}}(x+\ell)|_{t-} \end{cases},$$

$$x \in [2\ell, 3\ell] \quad \begin{cases} y_{\text{G},j}(x)|_{t+} = y_{\text{G},j}(x-2\ell)|_{t-} \\ T_{\text{G}}(x)|_{t+} = T_{\text{G}}(x-2\ell)|_{t-} \\ T_{\text{S}}(x)|_{t+} = T_{\text{S}}(x-2\ell)|_{t-} \end{cases}. \tag{16}$$

Velardi S., A. Barresi, D. Manca, D. Fissore, Chem. Eng. J., 99 117–123, 2004

Simulated Moving Bed Reactors

- After a suitable number of switches the temperature profile reaches a **pseudo-stationary** condition.

High switch times

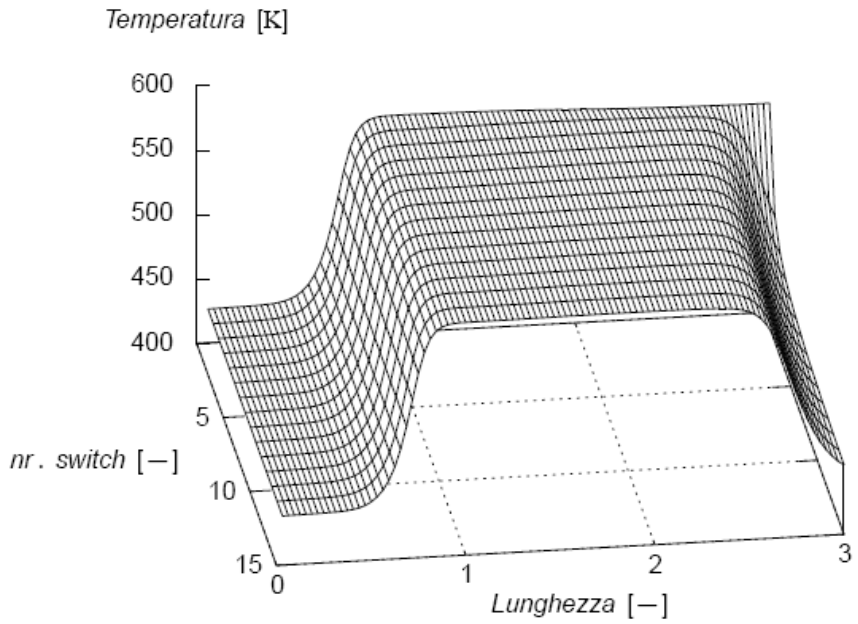

Low switch times

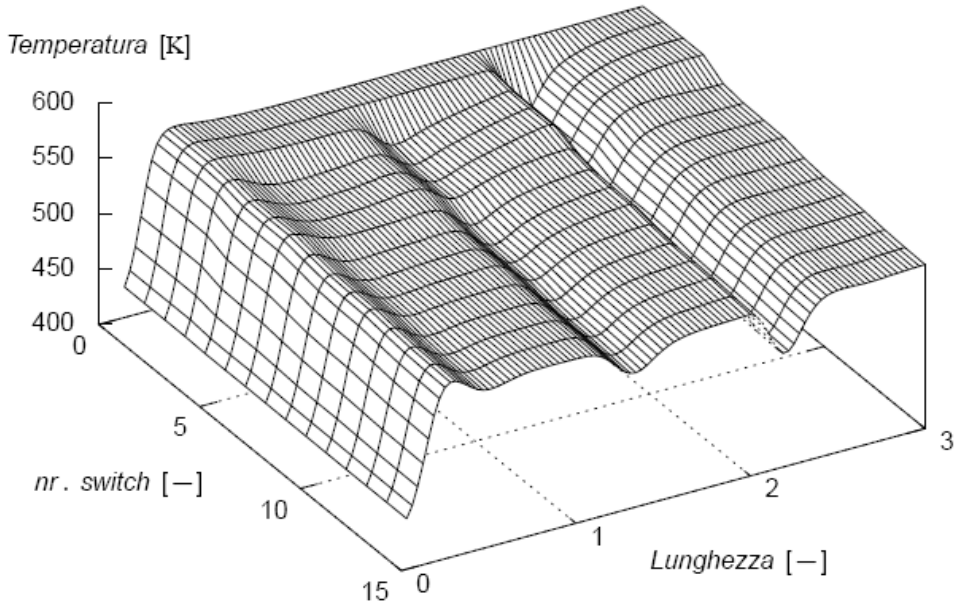

SMBR: the thermal wave

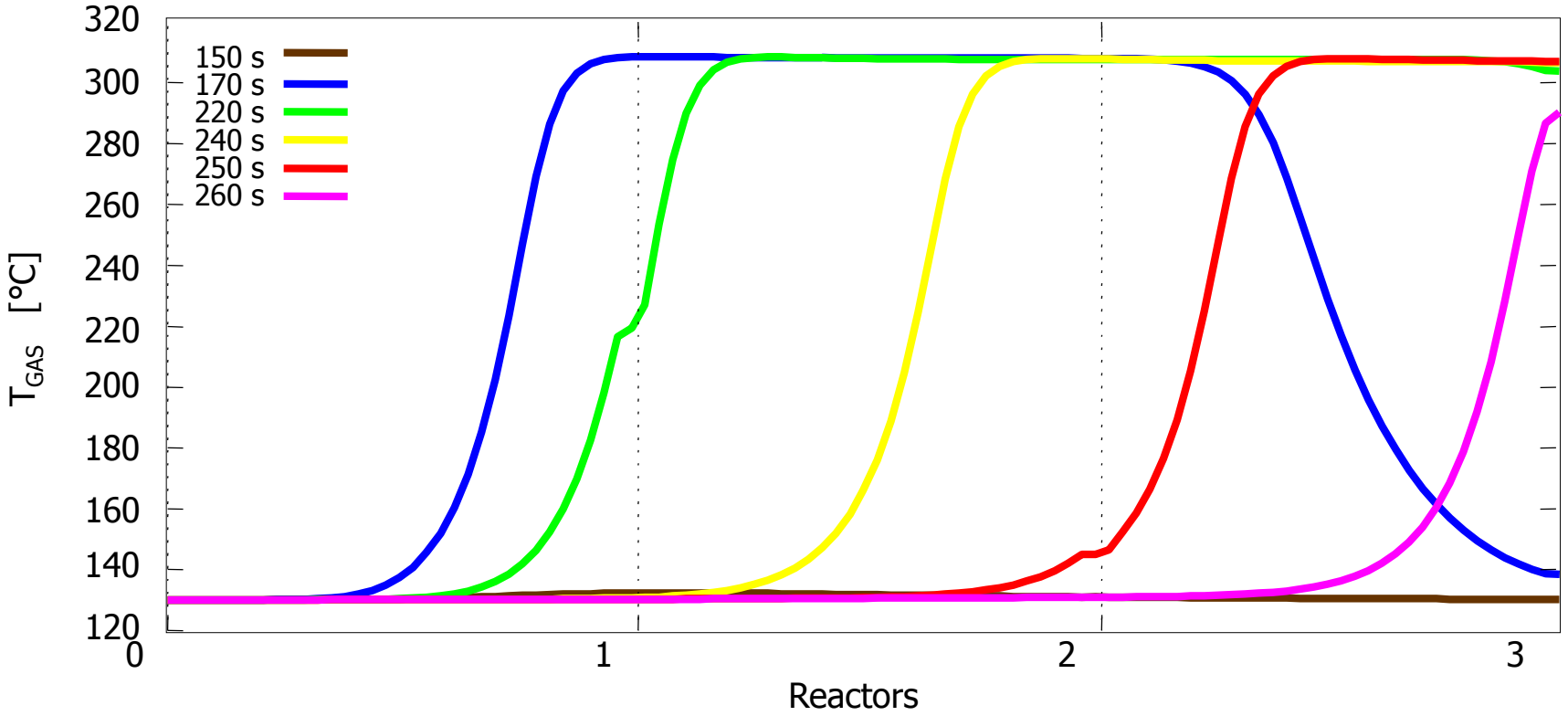

SMBR: open loop response

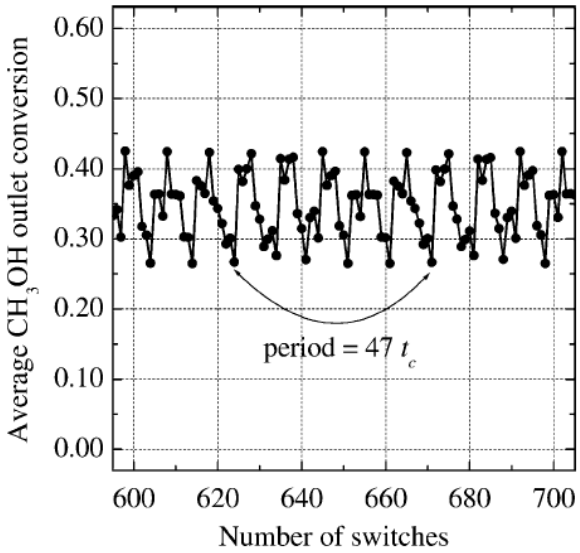

Fig. 5. Periodic evolution of the average methanol outlet conversion in the complex behaviour region; $t_c = 20\,s$, $T_{in} = 100\,°C$.

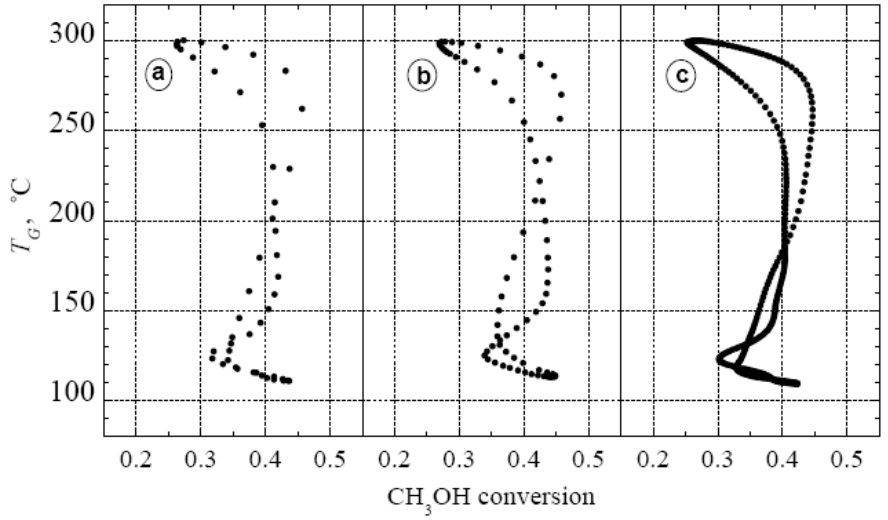

Fig. 6. Correlation between methanol conversion and the outlet gas temperature for different switching times. (a) Period $= 47t_c$, $t_c = 20\,s$; (b) period $= 72t_c$, $t_c = 22\,s$; (c) period $= 332\,t_c$, $t_c = 24\,s$. Points are taken in the middle of each cycle.

Velardi S., A. Barresi, D. Manca, D. Fissore, Chem. Eng. J., 99 117–123, 2004

SMBR: open loop response

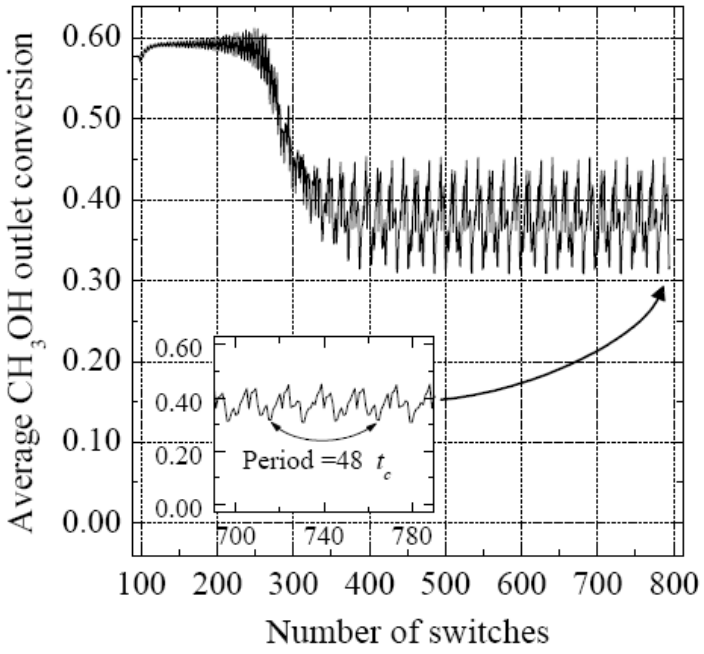

Fig. 7. Open loop response to a step disturbance $\Delta T_{G,in} = -10\,^{\circ}C$ and transition to a multi-periodic steady-state; $t_c = 40\,s$, $T_{in} = 130\,^{\circ}C$.

Velardi S., A. Barresi, D. Manca, D. Fissore, Chem. Eng. J., 99 117–123, 2004

SMBR: open loop response

Disturbance stop after **195** switches

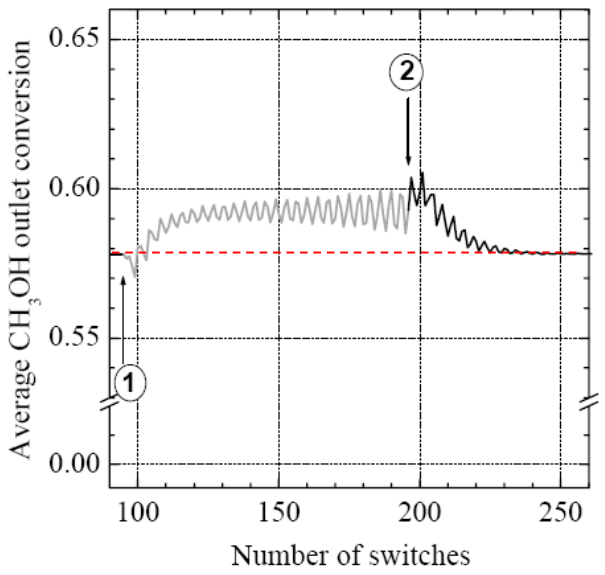

Fig. 8. Open loop response to a step disturbance $\Delta T_{G,in} = -10\,^{\circ}C$ (point 1) and restoration of the previous steady-state after the disturbance (point 2); $t_c = 40\,s$, $T_{in} = 130\,^{\circ}C$.

Disturbance stop after **310** switches

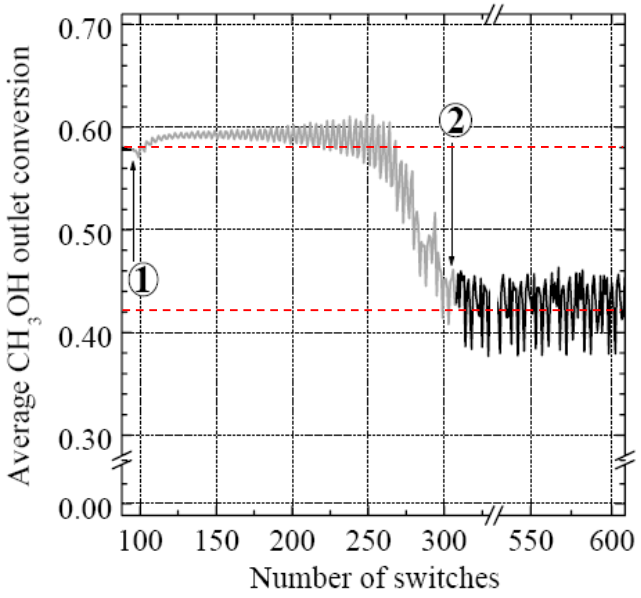

Fig. 9. Open loop response to a step disturbance $\Delta T_{G,in} = -10\,^{\circ}C$ (point 1) and new complex steady-state obtained when the conditions before the disturbance are restored (point 2); $t_c = 40\,s$, $T_{in} = 130\,^{\circ}C$.

There are more periodic stationary conditions

Velardi S., A. Barresi, D. Manca, D. Fissore, Chem. Eng. J., 99 117–123, 2004

The control problem

- **FEATURES**
  - The system may suddenly diverge to unstable operating conditions (even chaotic behavior);
  - The network may shut-down;
  - The reactors may work in a suboptimal region.
- **PROBLEM**
  - The reactor network should work within an optimal operating range;
  - Such a range is often narrow and its identification may be difficult.
- **SOLUTION**
  - A suitable control system must be synthesized and implemented on-line to avoid both shut-down and chaotic behaviors;
  - An advanced control system is highly recommended;
  - Model based control → Model Predictive Control, **MPC**.

Numerical modeling

- The model based approach to the control problem calls for the implementation of a **numerical model** of the network that will be used for:
  1. **Identification** of the optimal operating conditions;
  2. **Control purposes**, *i.e.* to predict the future behavior of the system.

- The numerical model is based on a first principles approach:
  - The reactors are continuously evolving (they never reach a steady-state condition) → time derivative;
  - Each PFR reactor must be described spatially → spatial derivative;
  - The reacting system is catalyzed (therefore it is heterogeneous). Consequently, an algebraic term is required → **PDAE system**.
  - The PDAE system is spatially discretized → **DAE system**.
  - A total of **1067 differential and algebraic equations** must be solved to determine the dynamic evolution of the network.

Mathematical tricks…

Stoichiometric closure:

$$y_{G,nComp} = 1 - \sum_{iComp=1}^{nComp-1} y_{G,iComp}$$

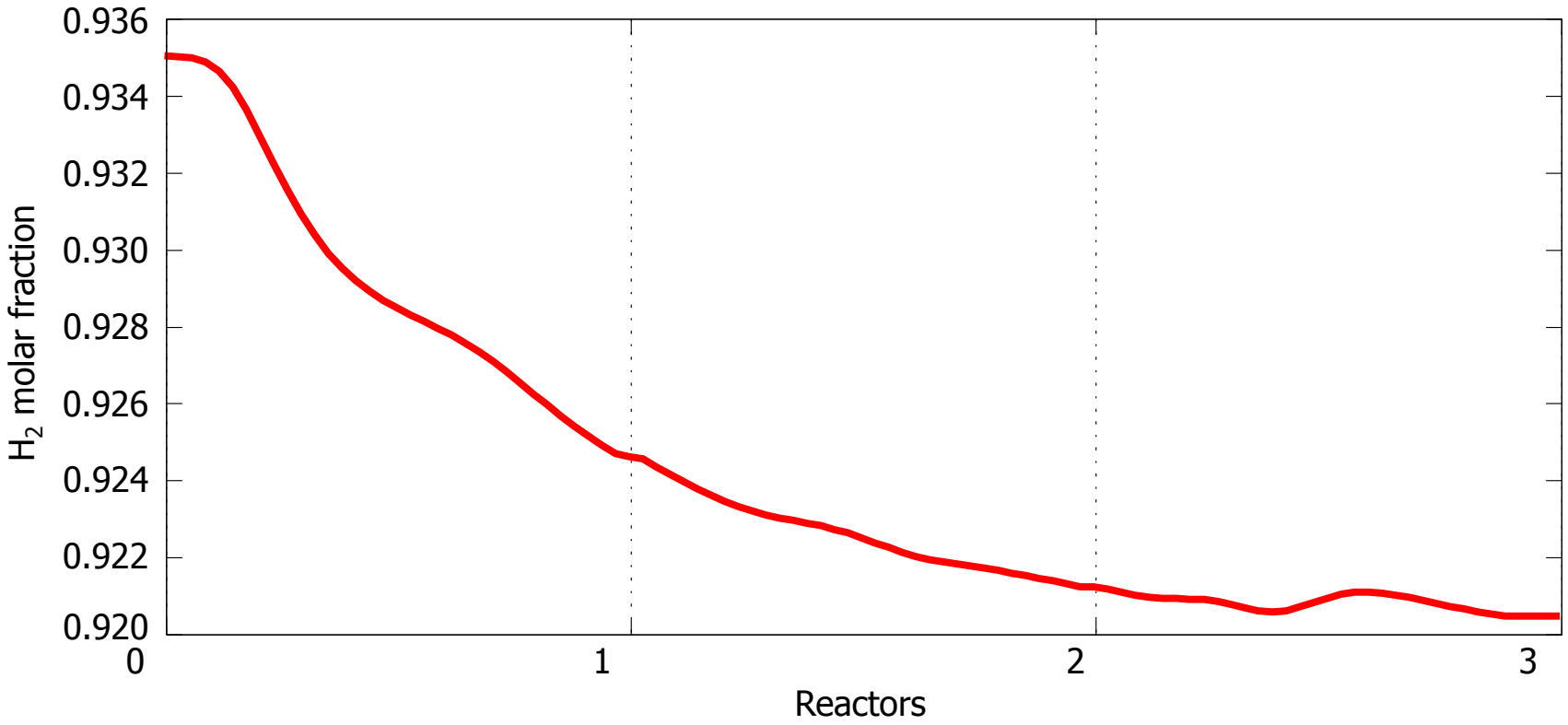

Numerical solution of the DAE

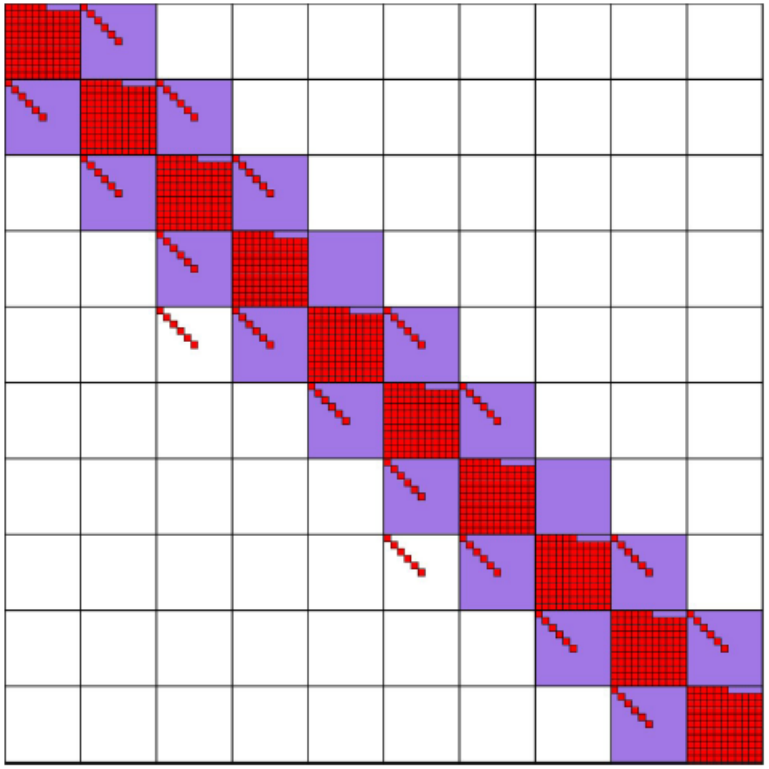

Boolean matrix that shows the presence indexes of the differential-algebraic system

Specifically tailored numerical algorithm for tridiagonal block systems

Numerical solution of the DAE

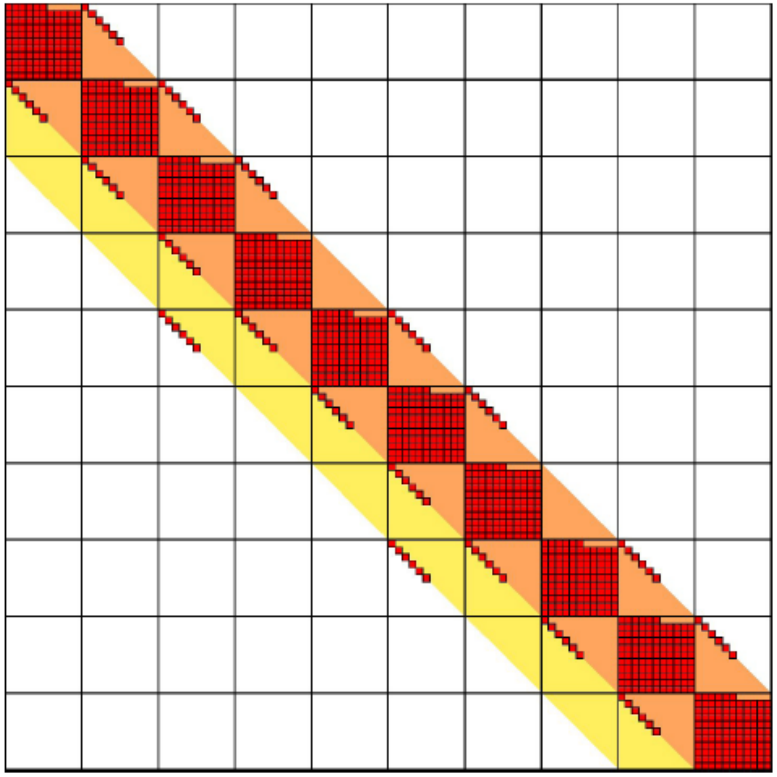

Boolean matrix that shows the presence indexes of the differential-algebraic system

Specifically tailored numerical algorithm for banded systems

Numerical solution of the DAE

BzzDAEFourBlocks

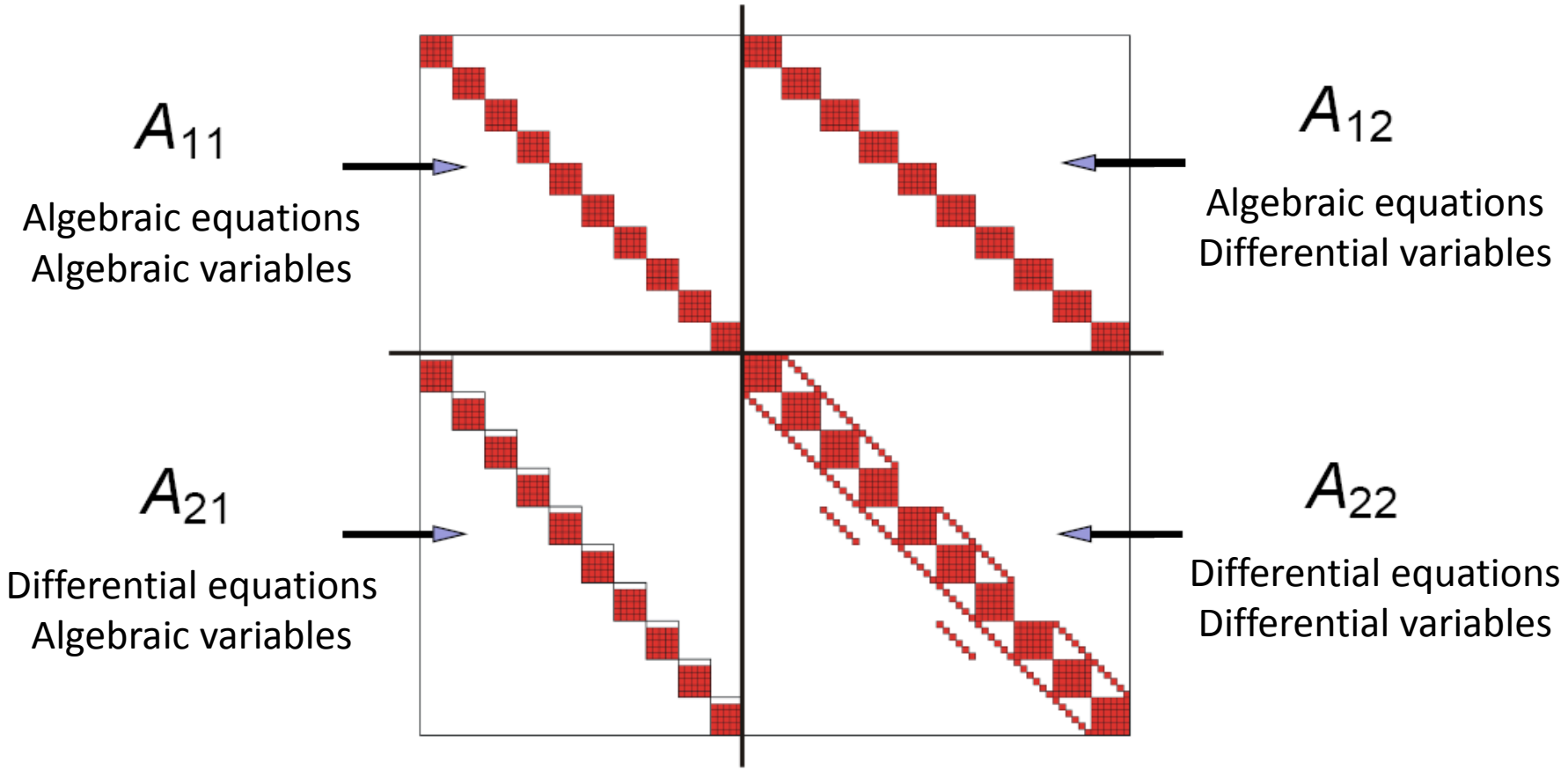

Numerical solution of the DAE

- Simulation time: 4000 s
- Switch time: 40 s
- Spatial discretization nodes: 97
- Number of equations per node: 11
- Total number of DAEs: 1067

- CPU: Intel® Pentium IV 2.4 GHz
- RAM: 512 MB
- OS: MS Windows 7 Professional
- Compiler: COMPAQ Visual Fortran 6.1 + MICROSOFT C++ 6.0

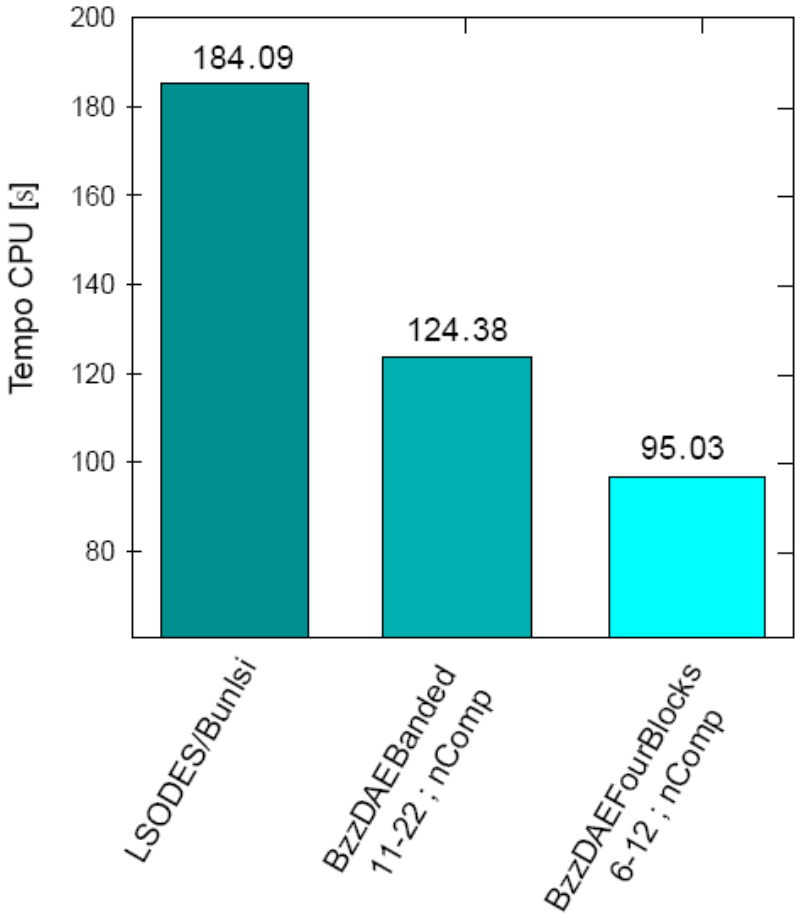

Numerical simulation

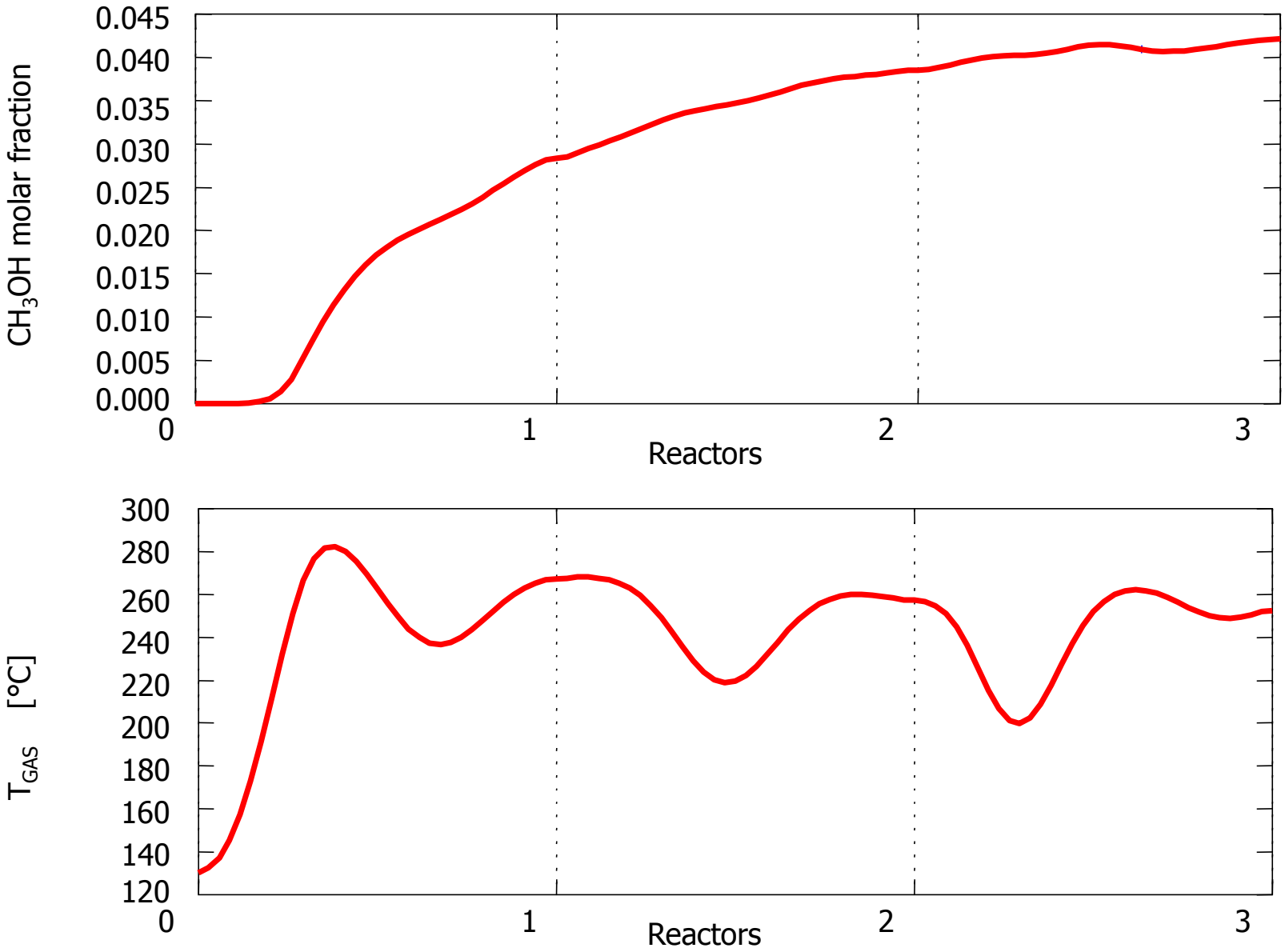

Numerical simulation

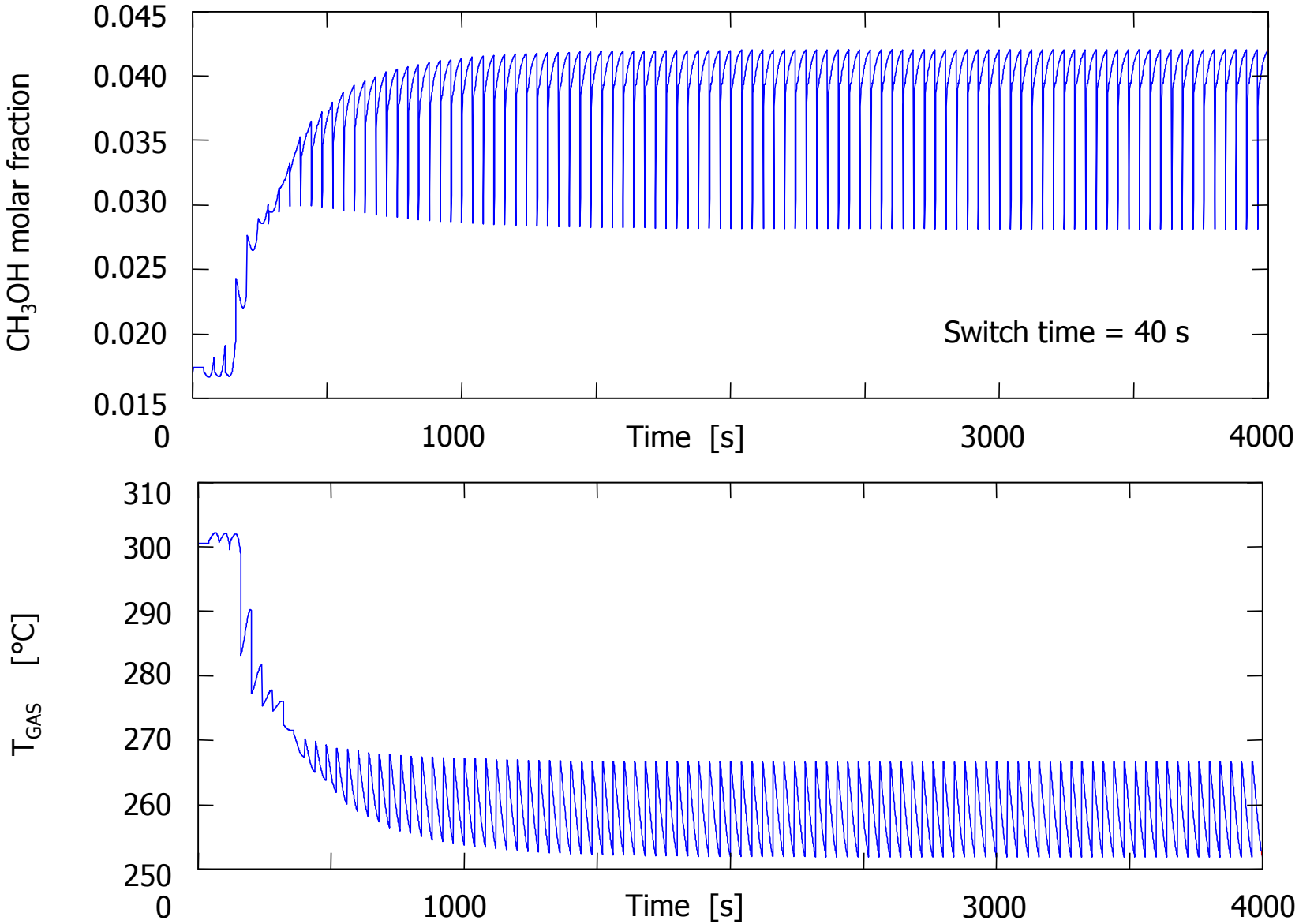

Parametric sensitivity study

- Variability interval of the analyzed process variables

Variable	Interval
Inlet gas temperature, T_{in} [K]	300÷593
Inlet gas velocity, v_{in} [m/s]	0.0189÷0.0231
Switch time, t_c [s]	1÷350

Parametric sensitivity study

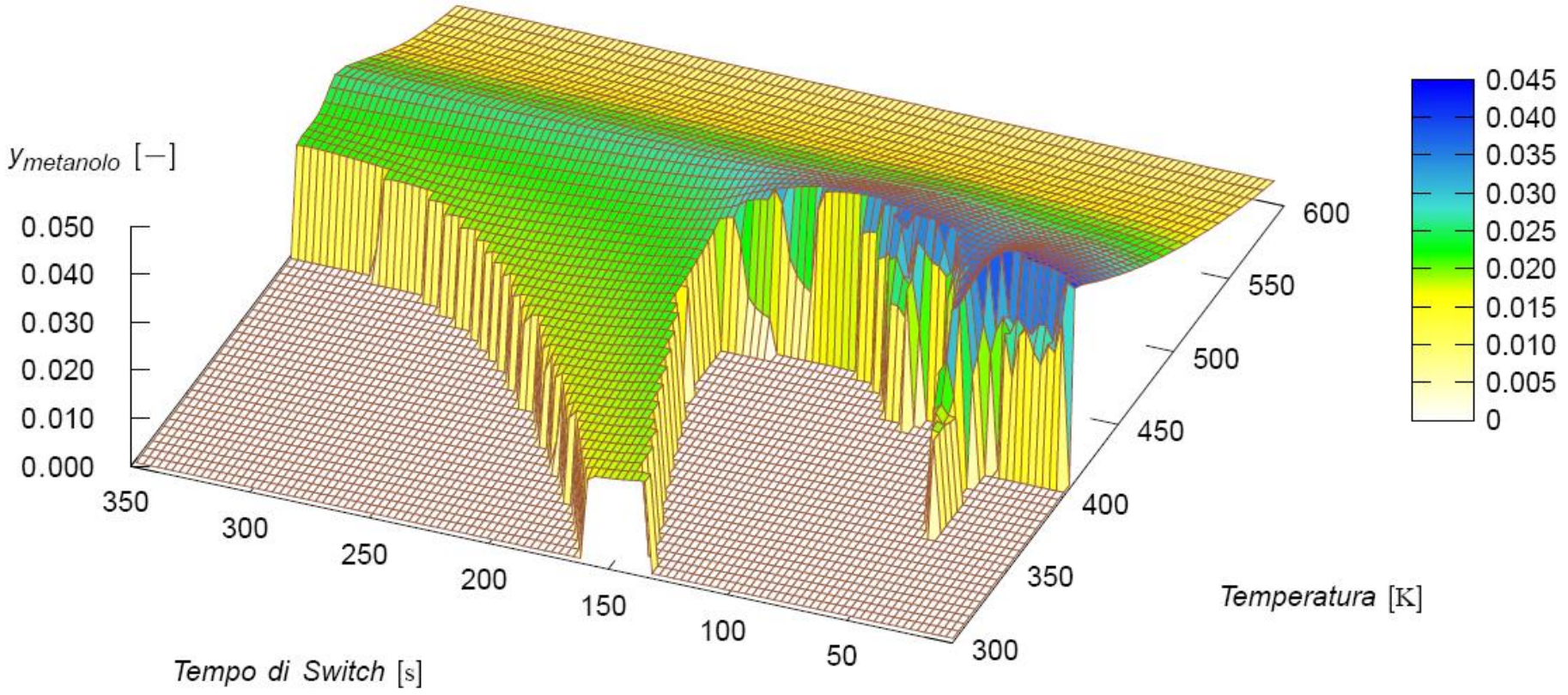

Parametric sensitivity study

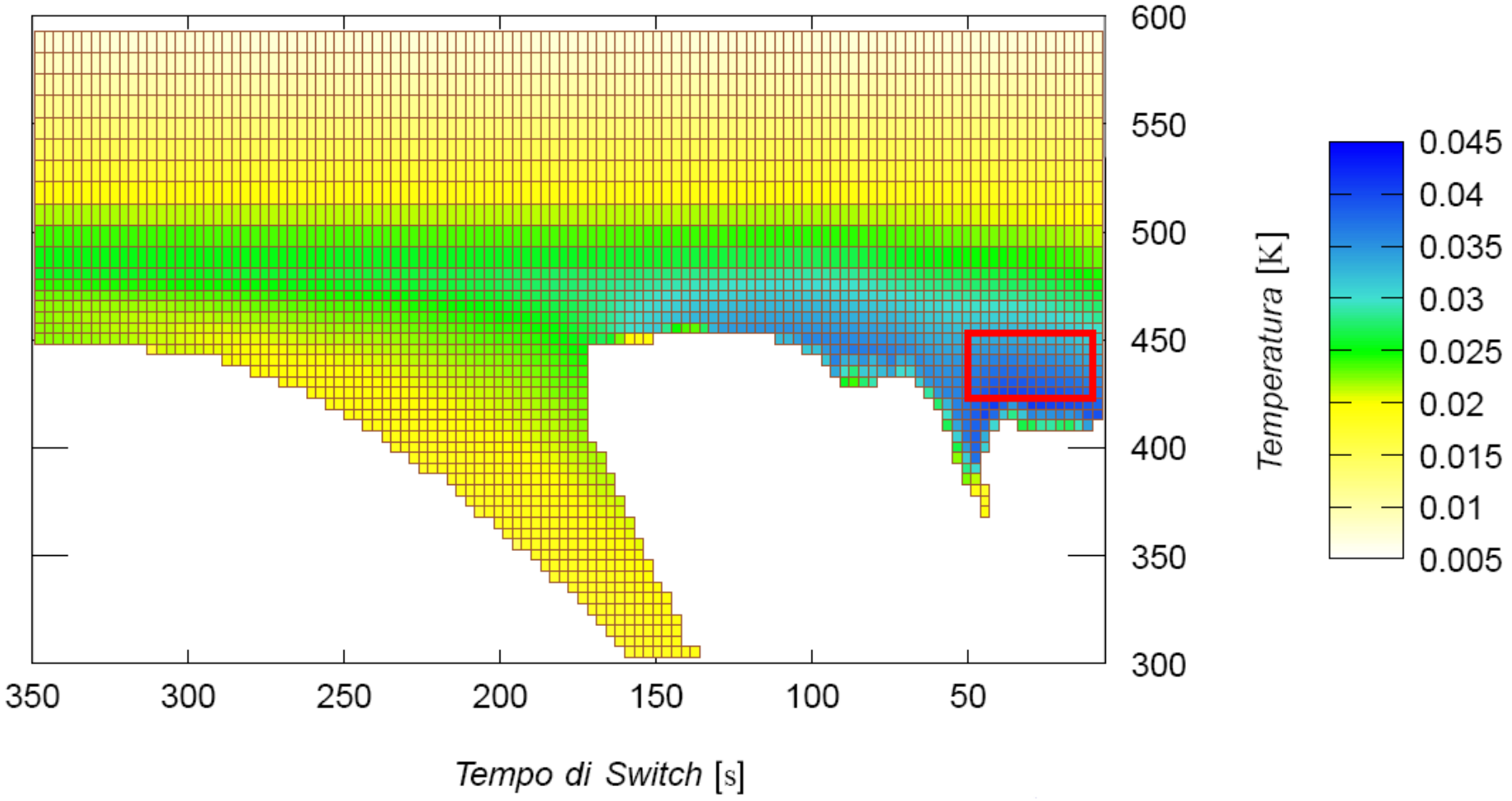

Parametric sensitivity study

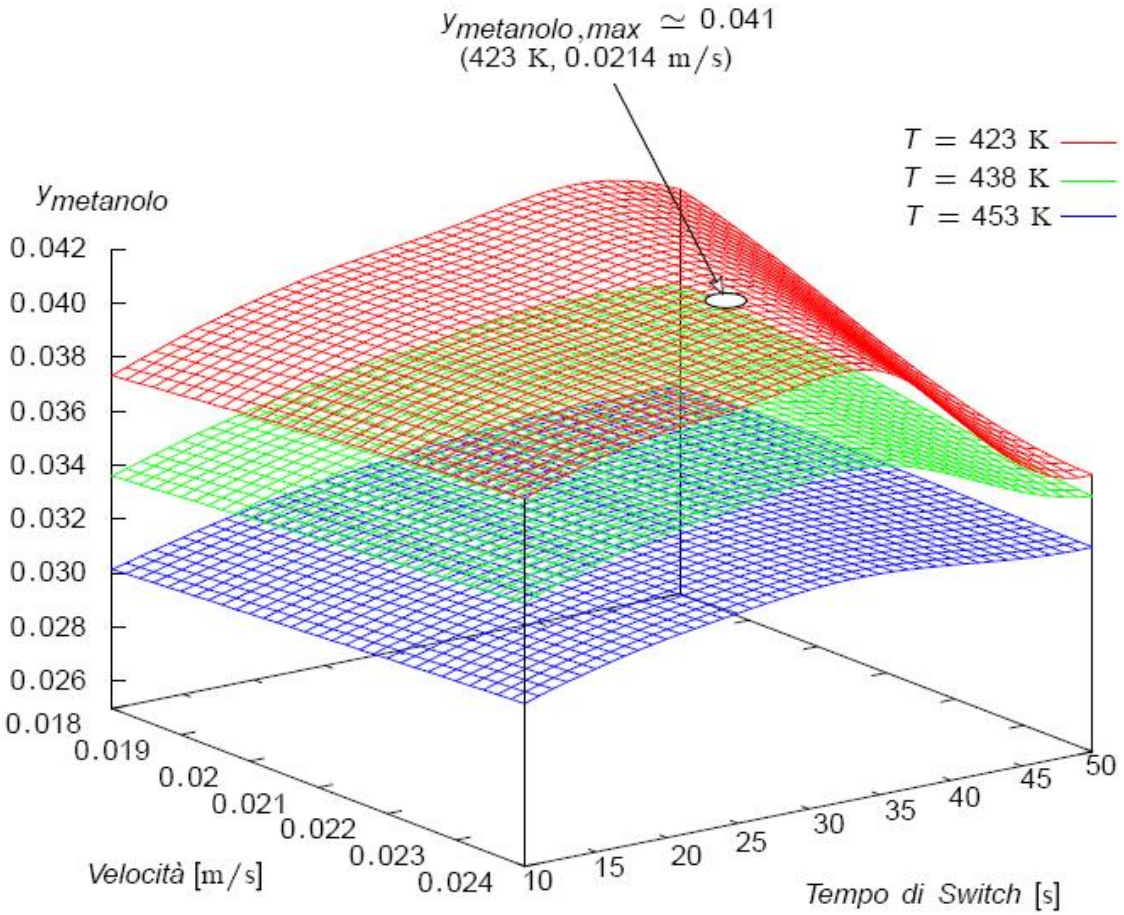

Need for speed

- **THE POINT**: to simulate 100 switches of the inlet flow with a switch time of 40 s (total of 4,000 s) the DAE system, comprising 1067 equations, takes about **95 s of CPU time** on a workstation computer.

- **PROBLEM**: the detailed first principles model requires a CPU time that is prohibitive for model based control purposes.

- **SOLUTION**
  - A **high efficiency** numerical model in terms of CPU time is therefore required;
  - Such a model should be able to describe the **nonlinearities** and the articulate profiles of the network of reactors;
  - Artificial Neural Networks, **ANN**, may be the answer.

System identification with ANN

ANN architecture

Input variables	Range
Inlet gas temperature, T_{in} [K]	423÷453
Inlet gas velocity, v_{in} [m/s]	0.0189÷0.0231
Switch time, t_c [s]	10÷50

Output variables
Mean methanol molar fraction, x_{CH3OH}
Outlet gas temperature, T_{GAS} [K]

ANN architecture

Levels		# of nodes	Activation function
1	Input	40	Sigmoid
2	Intermediate 1	15	Sigmoid
3	Intermediate 2	15	Sigmoid
4	Output	1	Linear
# of weights and biases		840 + 31 = **871**	
Learning factor, α		0.716	
Momentum, β		0.366	
Linear activation constant, μ		0.275	

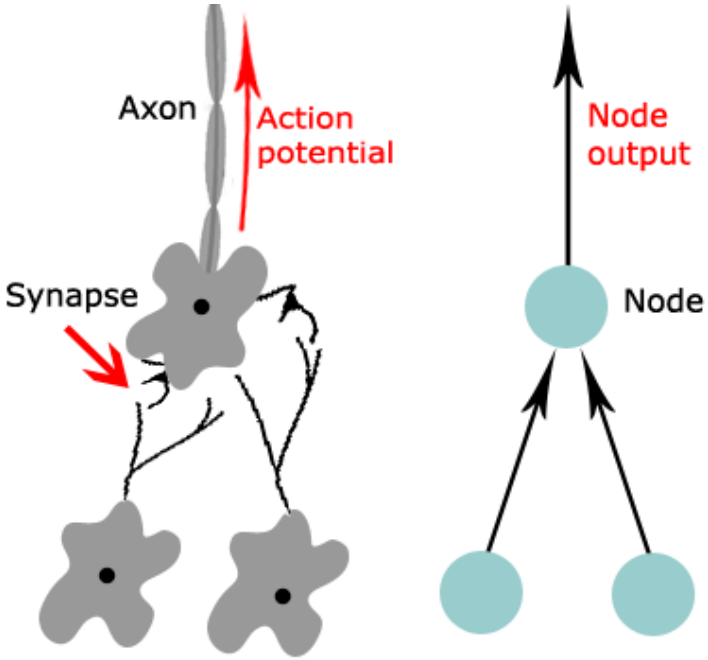

Random input patterns

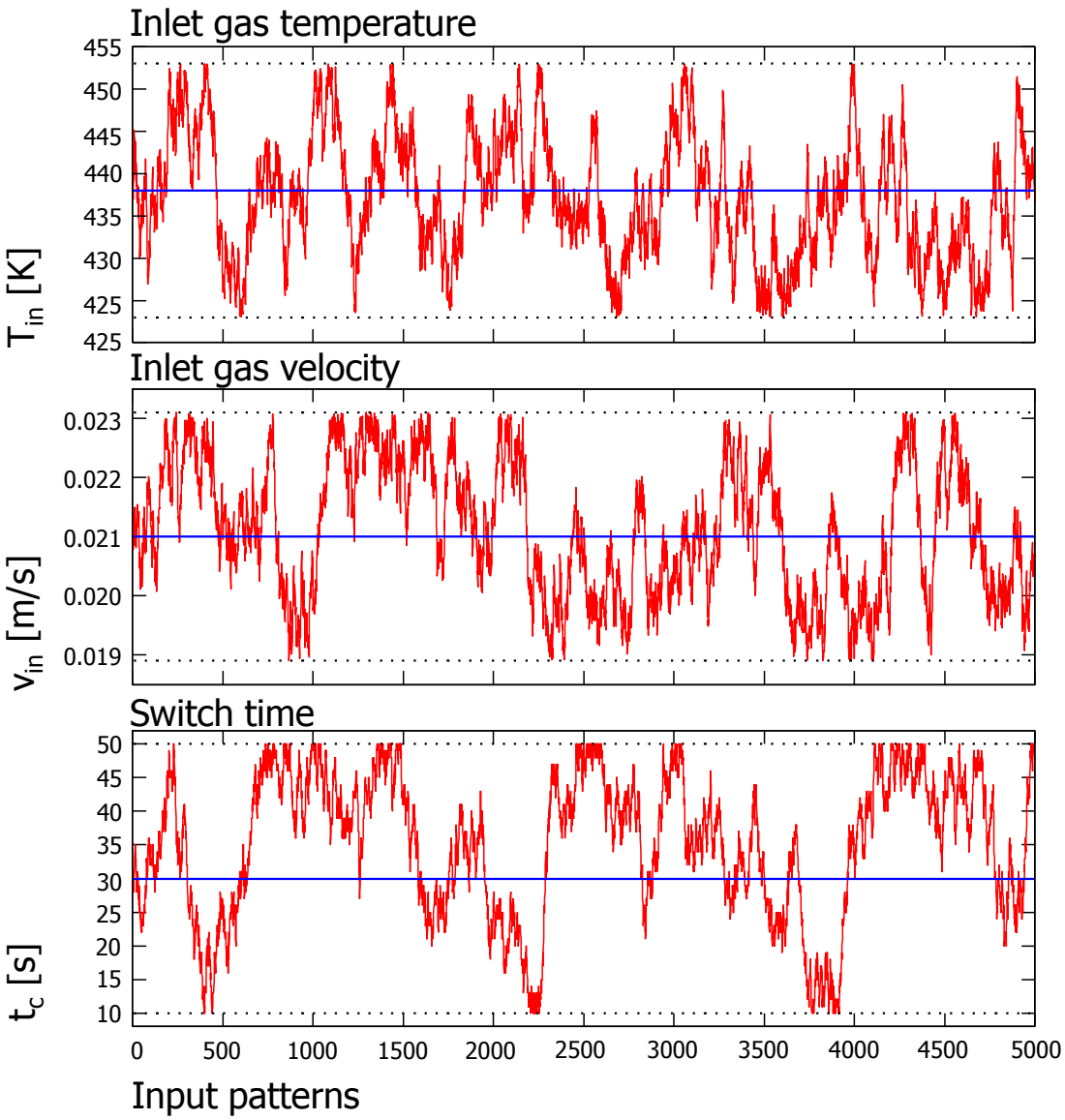

Levemberg Marquard learning algorithm

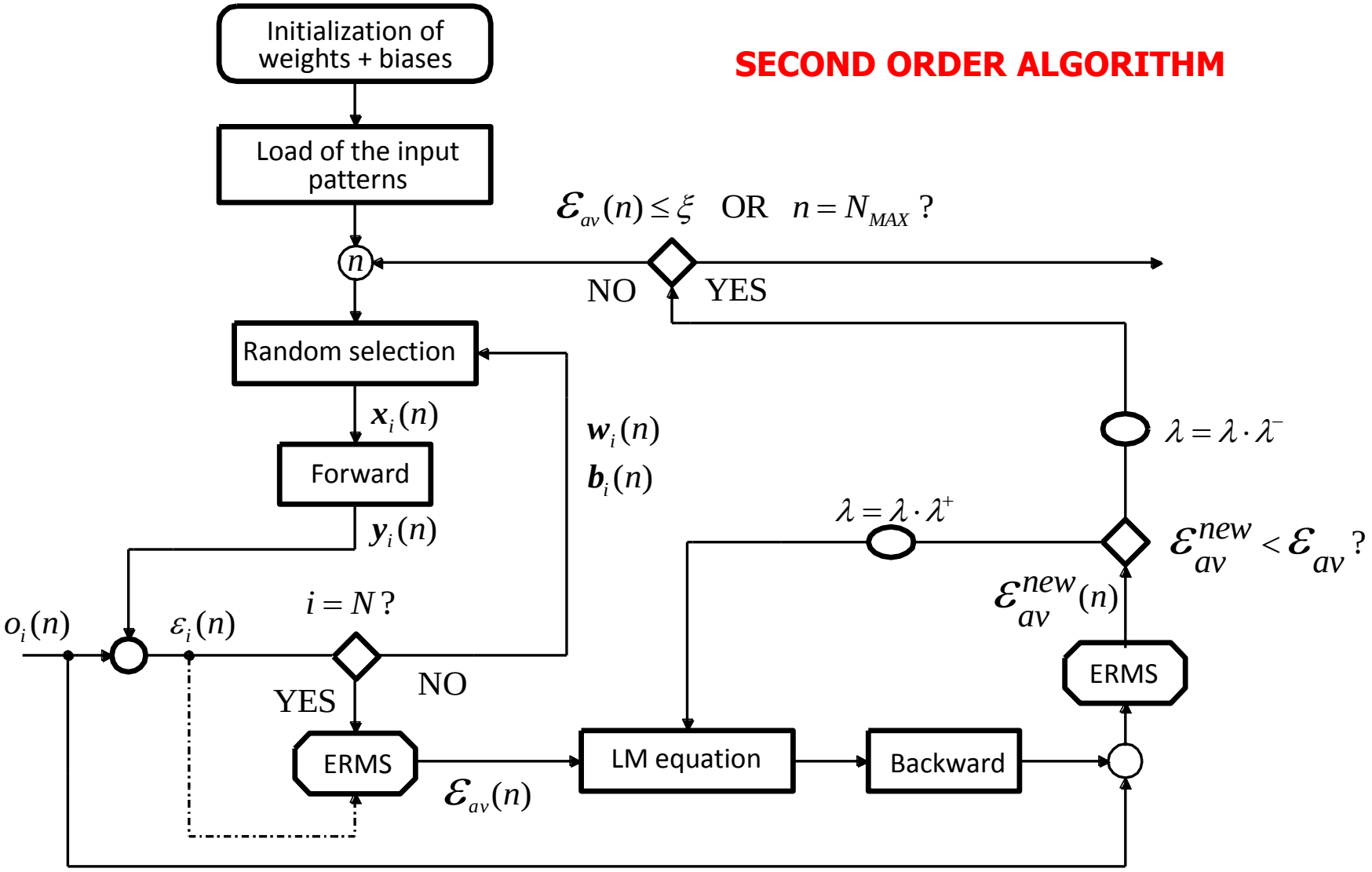

Algorithms comparison

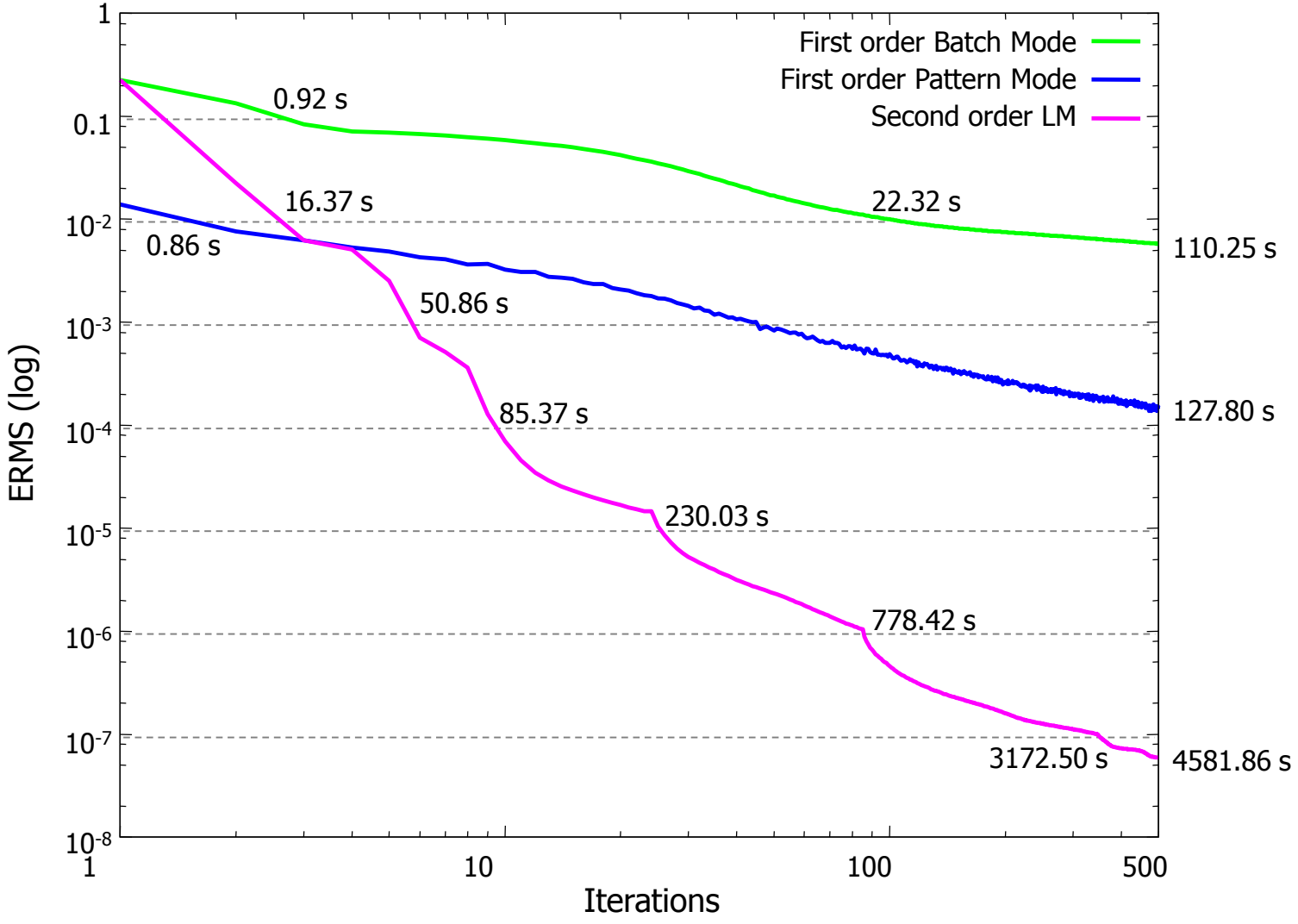

The overlearning problem

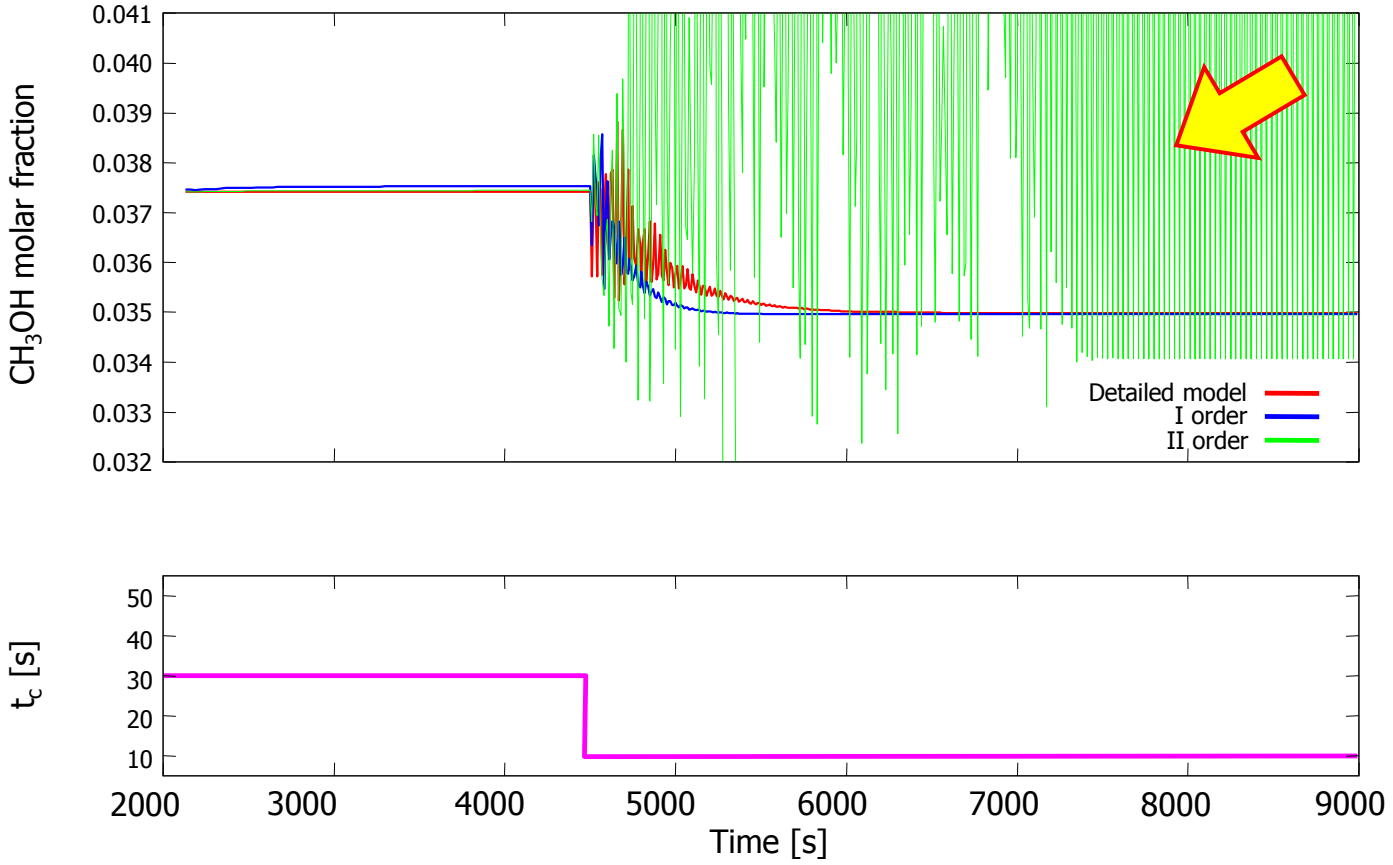

Disturbance on the **switch time** (from 30 to 10 s)

The overlearning problem

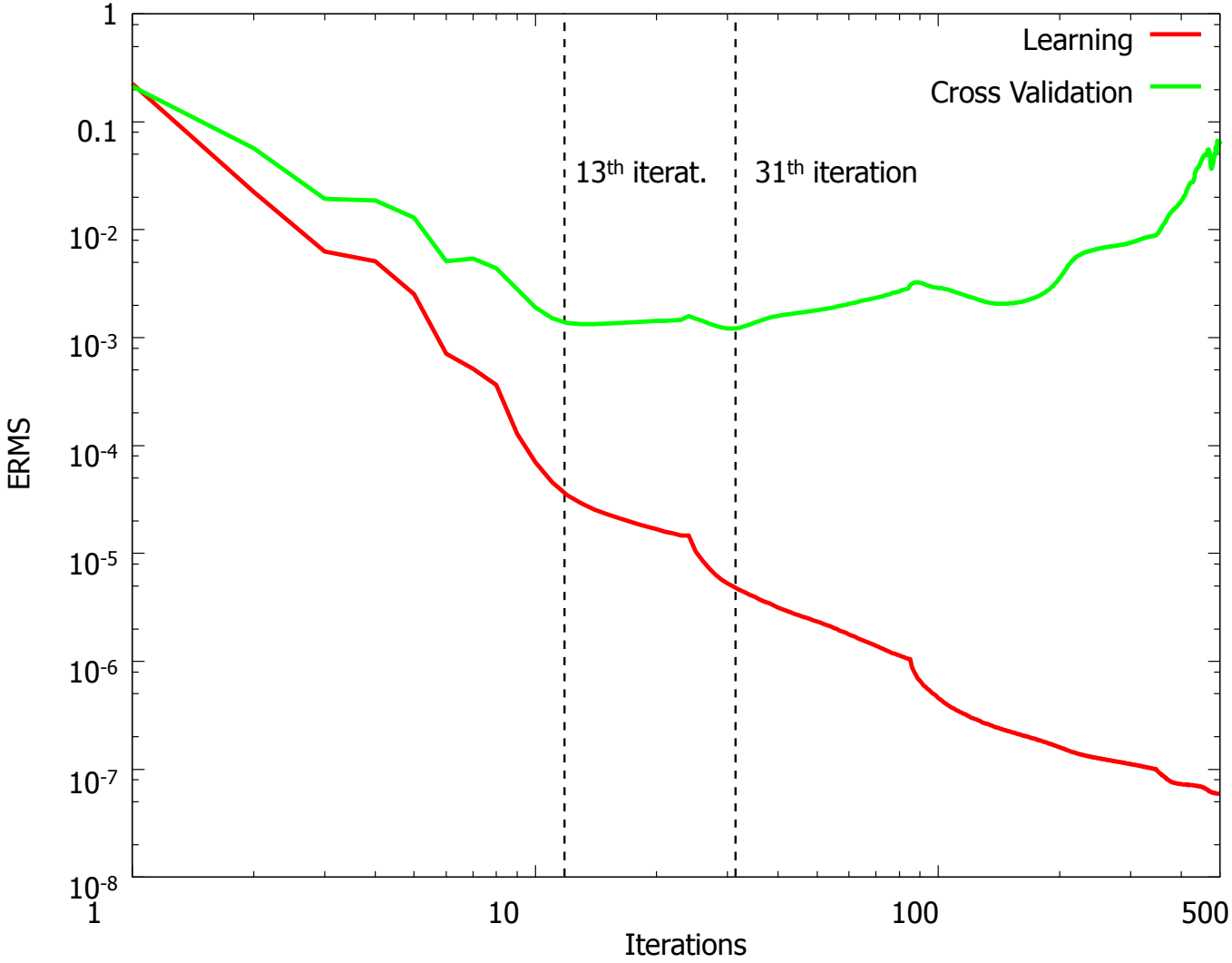

ANN cross-validation

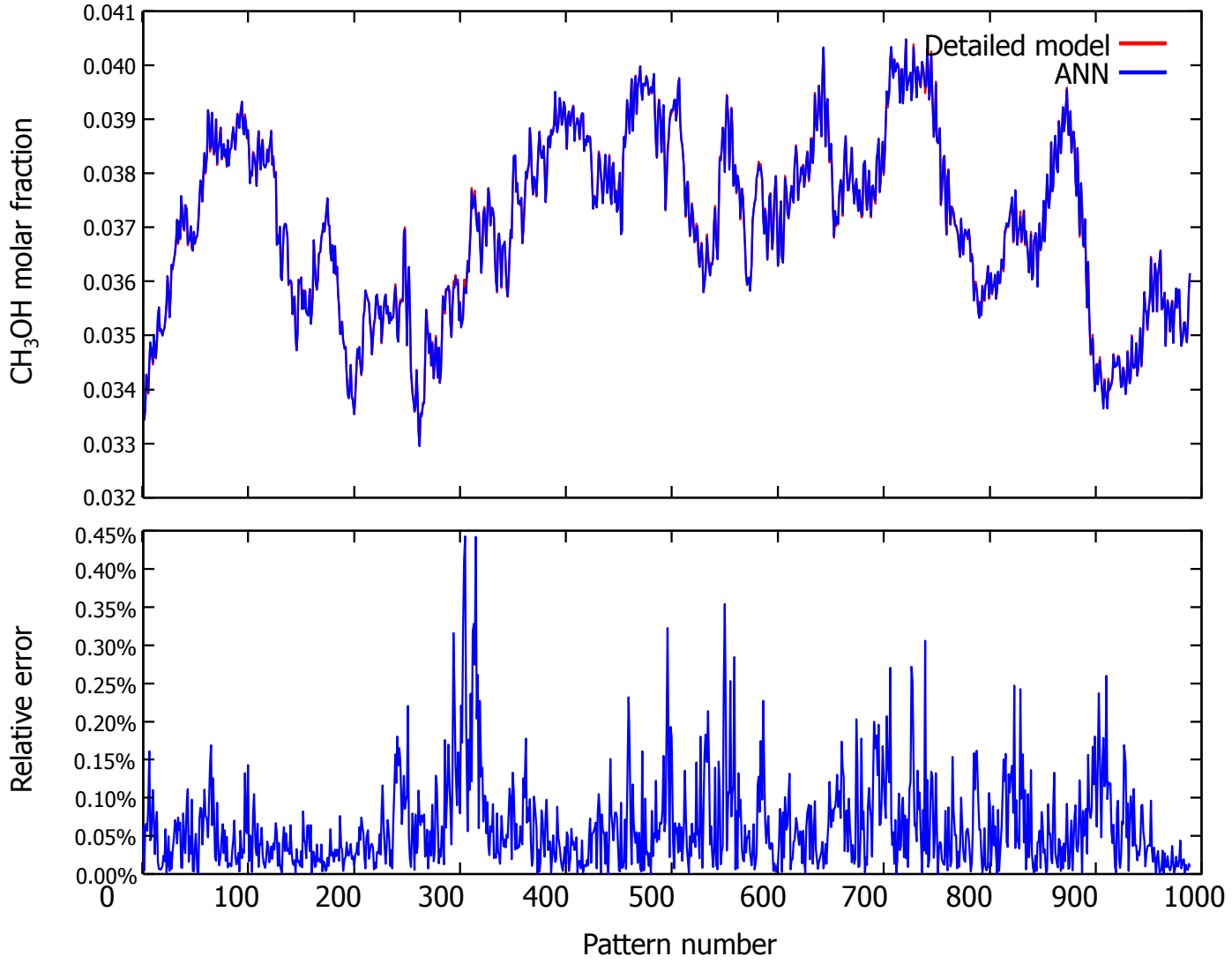

ANN disturbance response

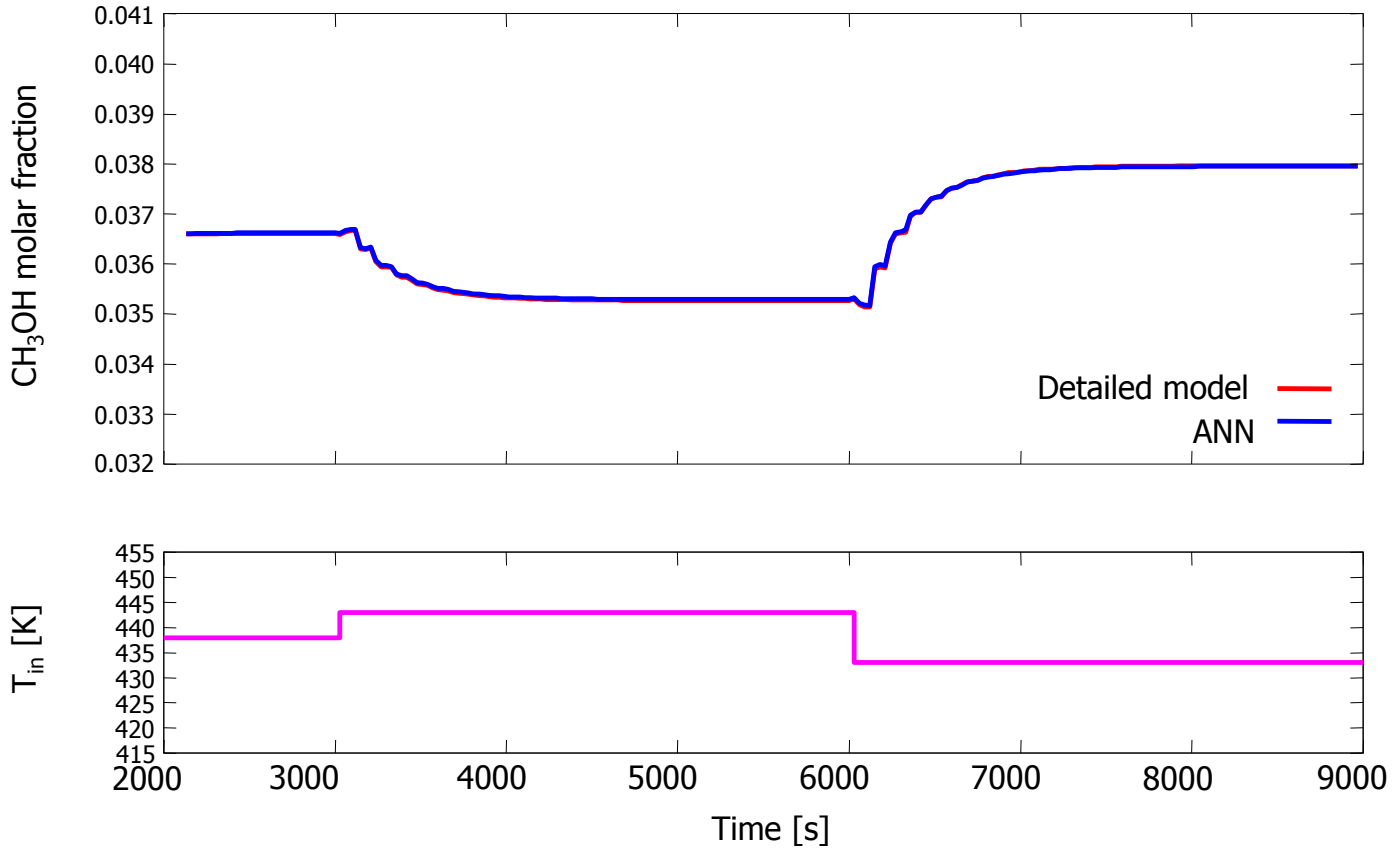

Disturbance on the **inlet temperature** 438 → 443 → 433 [K]

ANN disturbance response

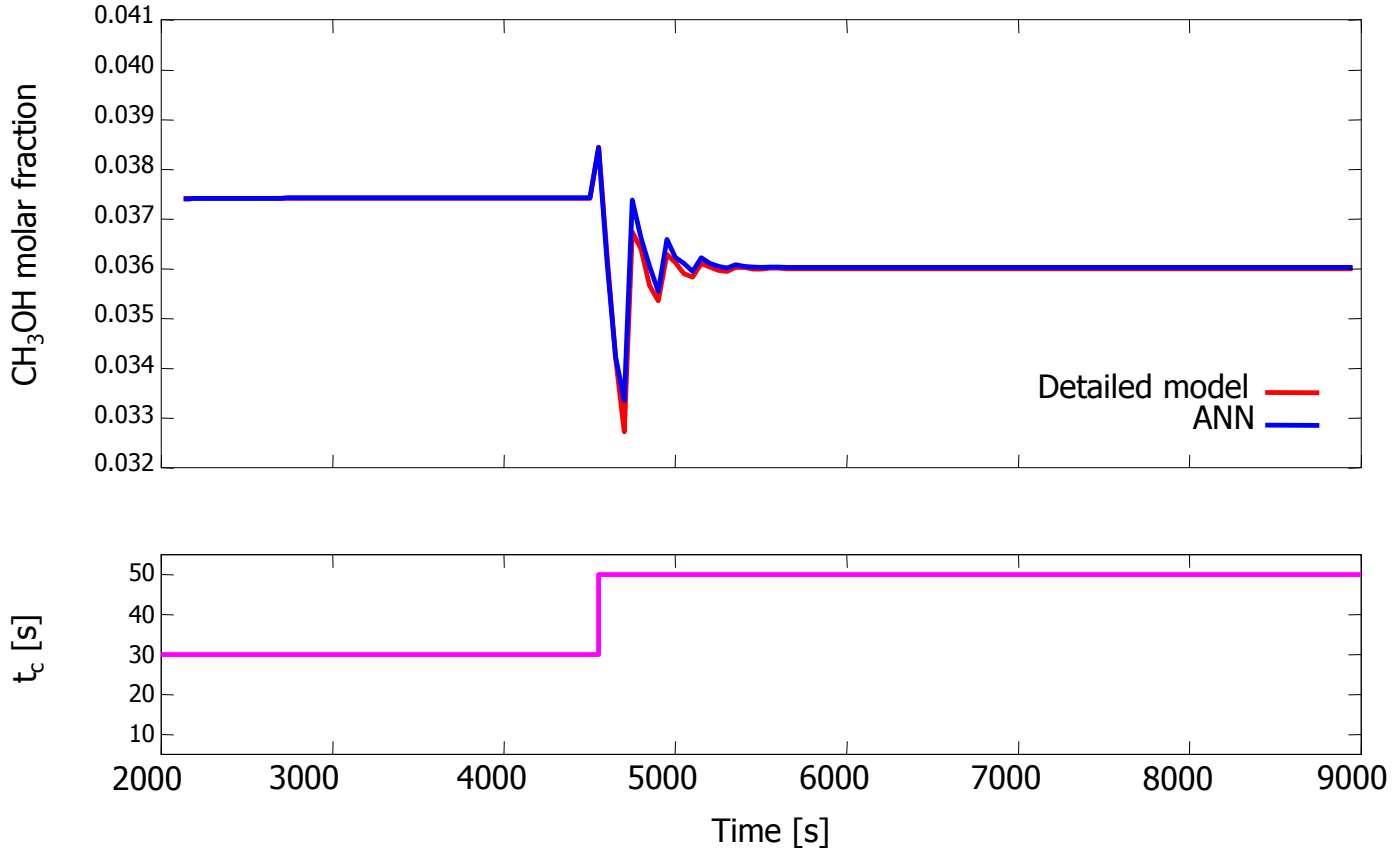

Disturbance on the **switch time** 30 → 45 [s]

ANN disturbance response

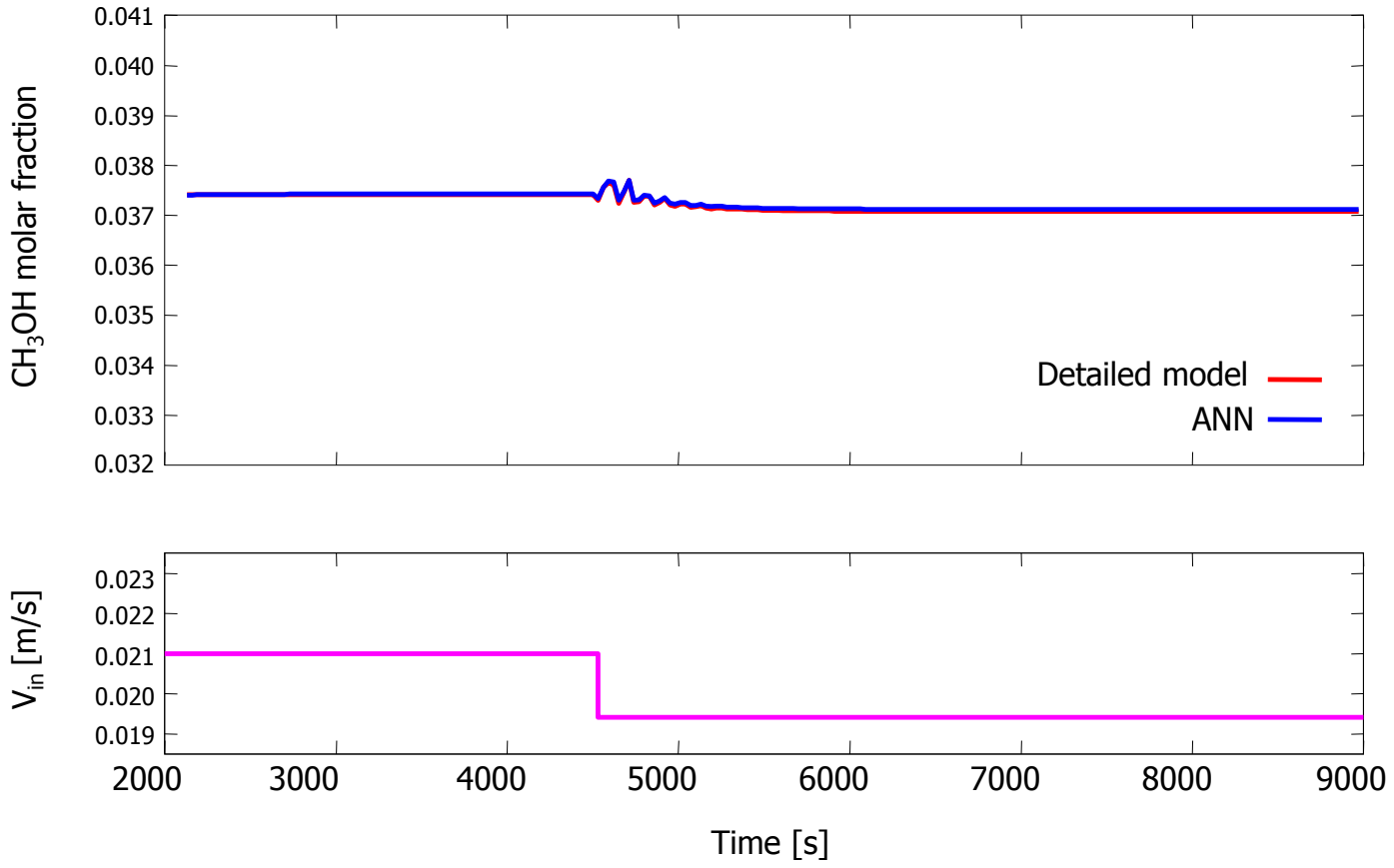

Disturbance on the **inlet velocity** 0.021 → 0.0194 [m/s]

ANN CPU times

	MISO		MIMO
ANN output variables	CH_3OH	T_G	CH_3OH+T_{GAS}
# of output nodes	1	1	2

# of weights and biases	840+31=871	840+31=871	855+32=887
Jacobian matrix dimensions	4000 x 871	4000 x 871	8000 x 887
CPU time for evaluating J^TJ [s]	17.38	17.37	49.13
Learning procedure CPU time	3h 14 min	3h 13 min	8 h 18 min

CPU time for a **single ANN simulation** [s]	**8.08E-6**	**8.23E-6**	**8.86E-6**

ABOUT 6 ORDERS OF MAGNITUDE IMPROVEMENT BETWEEN THE FIRST PRINCIPLES MODEL AND THE ANN

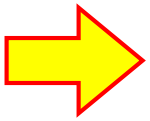

ON-LINE FEASIBILITY OF MODEL BASED CONTROL